20 Kamath, A. T., Feng, C. G., Macdonald, M., Briscoe, H. and Britton, W. J. 1999. Differential protective efficacy of DNA vaccines expressing secreted proteins of *Mycobacterium tuberculosis*. *Infect. Immun.* 67:1702.
21 Mustafa, A. S., Shaban, F. A., Abal, A. T., Al-Attiyah, R., Wiker, H. G., Lundin, K. E., Oftung, F. and Huygen, K. 2000. Identification and HLA restriction of naturally derived Th1-cell epitopes from the secreted *Mycobacterium tuberculosis* antigen 85B recognized by antigen-specific human $CD4^+$ T-cell lines. *Infect. Immun.* 68:3933.
22 Yanagisawa, S., Koike, M., Kariyone, A., Nagai, S. and Takatsu, K. 1997. Mapping of $V\beta11^+$ helper T cell epitopes on mycobacterial antigen in mouse primed with *Mycobacterium tuberculosis*. *Int. Immunol.* 9:227.
23 Kariyone, A., Higuchi, K., Yamamoto, S., Nagasaka-Kametaka, A., Harada, M., Takahashi, A., Harada, N., Ogasawara, K. and Takatsu, K. 1999. Identification of amino acid residues of the T-cell epitope of *Mycobacterium tuberculosis* α antigen critical for $V\beta11^+$ Th1 cells. *Infect. Immun.* 67:4312.
24 Kariyone, A., Tamura, T., Kano, H., Iwakura, Y., Takeda, K., Akira, S. and Takatsu, K. 2003. Immunogenicity of Peptide-25 of Ag85B in Th1 development: role of IFN-γ. *Int. Immunol.* 15:1183.
25 Ohno, H., Ushiyama, C., Taniguchi, M., Germain, R. N. and Saito, T. 1991. CD2 can mediate TCR/CD3-independent T cell activation. *J. Immunol.* 146:3742.
26 Morita, S., Kojima, T. and Kitamura, T. 2000. Plat-E: an efficient and stable system for transient packaging of retroviruses. *Gene Ther.* 7:1063.
27 Gyotoku, T., Fukui, Y. and Sasazuki, T. 1998. An endogenously processed self peptide and the corresponding exogenous peptide bound to the same MHC class II molecule could be distinct ligands for TCR with different kinetic stability. *Eur. J. Immunol.* 28:4050.
28 Kitamura, T., Koshino, Y., Shibata, F., Nakajima, H., Nosaka, T. and Kumagai, H. 2003. Retrovirus-mediated gene transfer and expression cloning, powerful tools in functional genomics. *Exp. Hematol.* 31:1007.
29 Yokosuka, T., Takase, K., Suzuki, M., Nakagawa, Y., Taki, S., Takahashi, H., Fujisawa, T., Arase, H. and Saito, T. 2002. Predominant role of T cell receptor (TCR)-α chain in forming preimmune TCR repertoire revealed by clonal TCR reconstitution system. *J. Exp. Med.* 195:991.
30 Pircher, H., Mak, T. W., Lang, R., Ballhausen, W., Ruedi, E., Hengartner, H., Zinkernagel, R. M. and Burki, K. 1989. T cell tolerance to Mlsa encoded antigens in T cell receptor Vβ8.1 chain transgenic mice. *EMBO J.* 8:719.
31 Hosken, N. A., Shibuya, K., Heath, A. W., Murphy, K. M. and O'Garra, A. 1995. The effect of antigen dose on $CD4^+$ T helper cell phenotype development in a T cell receptor-αβ-transgenic model. *J. Exp. Med.* 182:1579.
32 Abbas, A. K., Murphy, K. M. and Sher, A. 1996. Functional diversity of helper T lymphocytes. *Nature* 383:787.
33 O'Garra, A. 1998. Cytokines induce the development of functionally heterogeneous T helper cell subsets. *Immunity* 8:275.
34 Pfeiffer, C., Stein, J., Southwood, S., Ketelaar, H., Sette, A. and Bottomly, K. 1995. Altered peptide ligands can control CD4 T lymphocyte differentiation *in vivo*. *J. Exp. Med.* 181:1569.
35 Pernis, A., Gupta, S., Gollob, K. J., Garfein, E., Coffman, R. L., Schindler, C. and Rothman, P. 1995. Lack of interferon γ receptor beta chain and the prevention of interferon γ signaling in TH1 cells. *Science* 269:245.
36 Brombacher, F., Kastelein, R. A. and Alber, G. 2003. Novel IL-12 family members shed light on the orchestration of Th1 responses. *Trends Immunol.* 24:207.
37 Rulifson, I. C., Sperling, A. I., Fields, P. E., Fitch, F. W. and Bluestone, J. A. 1997. CD28 costimulation promotes the production of Th2 cytokines. *J. Immunol.* 158:658.
38 Kato, T. and Nariuchi, H. 2000. Polarization of naive $CD4^+$ T cells toward the Th1 subset by CTLA-4 costimulation. *J. Immunol.* 164:3554.
39 Salomon, B. and Bluestone, J. A. 1998. LFA-1 interaction with ICAM-1 and ICAM-2 regulates Th2 cytokine production. *J. Immunol.* 161:5138.
40 Smits, H. H., de Jong, E. C., Schuitemaker, J. H., Geijtenbeek, T. B., van Kooyk, Y., Kapsenberg, M. L. and Wierenga, E. A. 2002. Intercellular adhesion molecule-1/LFA-1 ligation favors human Th1 development. *J. Immunol.* 168:1710.
41 Ohshima, Y., Yang, L. P., Uchiyama, T., Tanaka, Y., Baum, P., Sergerie, M., Hermann, P. and Delespesse, G. 1998. OX40 costimulation enhances interleukin-4 (IL-4) expression at priming and promotes the differentiation of naive human $CD4^+$ T cells into high IL-4-producing effectors. *Blood* 92:3338.
42 Akiba, H., Miyahira, Y., Atsuta, M. *et al.* 2000. Critical contribution of OX40 ligand to T helper cell type 2 differentiation in experimental leishmaniasis. *J. Exp. Med.* 191:375.
43 Dong, C., Juedes, A. E., Temann, U. A., Shresta, S., Allison, J. P., Ruddle, N. H. and Flavell, R. A. 2001. ICOS co-stimulatory receptor is essential for T-cell activation and function. *Nature* 409:97.
44 Thierfelder, W. E., van Deursen, J. M., Yamamoto, K. *et al.* 1996. Requirement for Stat4 in interleukin-12-mediated responses of natural killer and T cells. *Nature* 382:171.
45 Kaplan, M. H., Sun, Y. L., Hoey, T. and Grusby, M. J. 1996. Impaired IL-12 responses and enhanced development of Th2 cells in Stat4-deficient mice. *Nature* 382:174.
46 Nakanishi, K., Yoshimoto, T., Tsutsui, H. and Okamura, H. 2001. Interleukin-18 regulates both Th1 and Th2 responses. *Annu. Rev. Immunol.* 19:423.
47 Szabo, S. J., Kim, S. T., Costa, G. L., Zhang, X., Fathman, C. G. and Glimcher, L. H. 2000. A novel transcription factor, T-bet, directs Th1 lineage commitment. *Cell* 100:655.
48 Mullen, A. C., High, F. A., Hutchins, A. S. *et al.* 2001. Role of T-bet in commitment of TH1 cells before IL-12-dependent selection. *Science* 292:1907.

JOURNAL OF CLINICAL MICROBIOLOGY, Nov. 2004, p. 5277–5285 Vol. 42, No. 11
0095-1137/04/$08.00+0 DOI: 10.1128/JCM.42.11.5277–5285.2004


# Dual-Probe Assay for Rapid Detection of Drug-Resistant *Mycobacterium tuberculosis* by Real-Time PCR

Takayuki Wada,[1] Shinji Maeda,[2]* Aki Tamaru,[3] Shigeyoshi Imai,[4] Atsushi Hase,[1] and Kazuo Kobayashi[2]

*Department of Microbiology, Osaka City Institute of Public Health and Environmental Sciences,[1] Department of Host Defense, Osaka City University Graduate School of Medicine,[2] Department of Microbiology, Osaka Prefectural Institute of Public Health,[3] and Central Clinical Laboratory, Osaka City University Hospital,[4] Osaka, Japan*

Received 24 March 2004/Returned for modification 9 May 2004/Accepted 11 July 2004

**Mutations in particular nucleotides of genes coding for drug targets or drug-converting enzymes lead to drug resistance in *Mycobacterium tuberculosis*. For rapid detection of drug-resistant *M. tuberculosis* in clinical specimens, a simple and applicable method is needed. Eight TaqMan minor groove binder (MGB) probes, which discriminate one-base mismatches, were designed (dual-probe assay with four reaction tubes). The target of six MGB probes was the *rpoB* gene, which is involved in rifampin resistance; five probes were designed to detect for mutation sites within an 81-bp hot spot of the *rpoB* gene, and one probe was designed as a tuberculosis (TB) control outside the *rpoB* gene hot-spot. We also designed probes to examine codon 315 of *katG* and codon 306 of *embB* for mutations associated with resistance to isoniazid and ethambutol, respectively. Our system was *M. tuberculosis* complex specific, because neither nontuberculous mycobacteria nor bacteria other than mycobacteria reacted with the system. Detection limits in direct and preamplified analyses were 250 and 10 fg of genomic DNA, respectively. The system could detect mutations of the *rpoB*, *katG*, and *embB* genes in DNAs extracted from 45 laboratory strains and from sputum samples of 27 patients with pulmonary TB. This system was much faster (3 h from DNA preparation) than conventional drug susceptibility testing (3 weeks). Results from the dual-MGB-probe assay were consistent with DNA sequencing. Because the dual-probe assay system is simple, rapid, and accurate, it can be applied to detect drug-resistant *M. tuberculosis* in clinical laboratories.**

Tuberculosis (TB) presents a significant health threat to the world's population, with 8 million new cases of disease and 2 million deaths per year (36). To minimize the emergence and spread of drug-resistant TB, the basic principle of anti-TB treatment is to administer multiple drugs to which the organism is susceptible. Strains of *Mycobacterium tuberculosis* that are resistant to anti-TB drugs are being encountered with increased frequency (7). The major risk factors for drug resistance include inadequate prescription and delivery of chemotherapy, poor compliance, and an insufficient number of active drugs in the treatment regimen. The emergence of drug-resistant strains threatens our capability to control TB (2). Multidrug-resistant (MDR) *M. tuberculosis*, defined as simultaneous resistance to at least isoniazid (INH) and rifampin (RIF), is a serious problem. Strains of MDR *M. tuberculosis* appear to result from the stepwise acquisition of mutations in the genes encoding drug targets or drug-converting enzymes (10).

Rapid detection of susceptibility or resistance is crucial for TB treatment, because the initial choice of effective drugs is important. Major anti-TB drugs include INH, RIF, and ethambutol (EMB). Genetic studies have demonstrated that more than 95% of RIF resistance is associated with a mutation in the 81-bp core region of the *rpoB* gene (26, 31). RIF-susceptible mycobacteria do not possess the known mutations in core region of the *rpoB* gene. Therefore, mutations in the *rpoB* gene indicate that bacteria are RIF resistant. By contrast, INH-resistant strains exhibit mutations in several genes, such as *katG*, *inhA*, *oxyR*, and *ahpC* (22, 27, 30). The mutation of codon 315 (Ser) in the catalase-peroxidase (*katG*) gene is the most frequent site (30 to 65% of resistant strains) (4, 11). Furthermore, EMB-resistant strains have a point mutation at codon 306 (Met) in *embB* (3, 28), and the frequency is about 70% (3). Mutations of these sites are merely one mechanism leading to drug resistance. Many clinical isolates of drug-resistant *M. tuberculosis* do not bear mutations in these sites. Even if all of these mutations are examined, some resistant bacteria remain undetectable. However, the presence of mutations in the sites indicates that these bacilli are drug resistant (sensitivity, <100%; positive predictive value, 100%). In drug susceptibility testing, the culture method remains the "gold standard" (15). Since culture requires at least 2 weeks to obtain results (20), rapid diagnosis of drug resistance provides new opportunities for chemotherapeutic intervention in TB.

Because TaqMan minor groove binder (MGB) probes can distinguish one-base mismatches, the real-time PCR system in combination with MGB probes has been applied to analyze single-nucleotide polymorphisms (1, 12). It has been proven that the specificity of MGB probes is quite high (18). In the present study, we have developed a real-time PCR-based system with TaqMan MGB probes to detect the mutations asso-

* Corresponding author. Mailing address: Department of Host Defense, Osaka City University Graduate School of Medicine, 1-4-3 Asahi-machi, Abeno-ku, Osaka 545-8585, Japan. Phone: 81-6-6645-3746. Fax: 81-6-6645-3747. E-mail: smaeda@med.osaka-cu.ac.jp.

ciated with resistance of *M. tuberculosis* to INH, RIF, and EMB.

## MATERIALS AND METHODS

**Bacterial strains.** To confirm the specificity of the real-time PCR system, we used DNAs extracted from *M. tuberculosis* H37Rv (ATCC 25618), *Mycobacterium bovis* (Ravenel), *M. bovis* BCG (Tokyo), *Mycobacterium africanum* (ATCC 25420), *Mycobacterium microti* (TC 77), *Mycobacterium avium* (ATCC 15769), *Mycobacterium intracellulare* (ATCC 13950), *Mycobacterium kansasii* (ATCC 12478), *Mycobacterium marinum* (ATCC 927), *Mycobacterium simiae* (ATCC 25275), *Mycobacterium asiaticum* (ATCC 25276), *Mycobacterium xenopi* (ATCC 19250), *Mycobacterium scrofulaceum* (ATCC 19981), *Mycobacterium gordonae* (ATCC 14470), *Mycobacterium malmoense* (ATCC 29571), *Mycobacterium shimoidei* (ATCC 27962), *Mycobacterium nonchromogenicum* (ATCC 19530), *Mycobacterium fortuitum* (ATCC 6841), *Mycobacterium abscessus* (ATCC 19977), *Mycobacterium tokaiense* (ATCC 27282), *Mycobacterium austroafricanum* (ATCC 33464), *Mycobacterium pulveris* (ATCC 35154), *Mycobacterium smegmatis* (ATCC 14468), and *Mycobacterium leprae* (Thai 53). *M. leprae* was a kind gift from M. Matsuoka, Leprosy Research Center, National Institute of Infectious Diseases, Tokyo, Japan. In addition to mycobacteria, DNAs from *Klebsiella pneumoniae* (clinical isolate), *Pseudomonas aeruginosa* (ATCC 27853), and *Staphylococcus aureus* (ATCC 29213) were used.

**Drug-resistant clinical isolates and DNA isolation.** Using the proportion method with Ogawa egg medium, drug resistance was defined as growth of at least 1% of the number of colonies that grew on drug-free medium at critical concentrations of the drugs (i.e., 40 mg of RIF per liter, 0.2 mg of INH per liter, and 2 mg of EMB per liter) (35). The present study examined 45 laboratory strains of RIF-resistant *M. tuberculosis* (resistant to RIF alone, 7 strains; resistant to RIF and INH, 12 strains; resistant to RIF and EMB, 9 strains; resistant to RIF, INH, and EMB, 17 strains). Genomic DNAs of mycobacteria were isolated from bacteria grown on Ogawa medium by combined chloroform extraction and mechanical disruption (16). DNAs from *K. pneumoniae*, *P. aeruginosa*, and *S. aureus* were extracted with a QIAamp DNA Mini kit (Qiagen Inc., Valencia, Calif.). DNA concentration was estimated by UV absorbance at 260 nm.

**Clinical samples and DNA preparation.** We examined 27 clinical samples of sputum from patients with pulmonary TB. Drug susceptibility testing was performed as described in a previous study (35). A concentrated smear was prepared from specimens that were decontaminated by using the N-acetyl-L-cysteine–NaOH protocol (17). The basic fuchsin (Ziehl-Neelsen) staining procedure was employed. The DNAs were extracted by using the AMPLICOR respiratory specimen preparation kit (Roche Diagnostic Systems, Inc., Branchburg, N.J.) according to the manufacturer's instructions and were confirmed as *M. tuberculosis* complex with the COBAS AMPLICOR *M. tuberculosis* detection kit (Roche Diagnostic Systems, Inc.) (25).

**PCR amplification and DNA sequencing.** DNA sequences of *rpoB* (GenBank accession no. L27989), *embB* (U68480), and *katG* (X68081) were used for primer design. PCR was performed with each primer set (Table 1) as described previously (19). Both strands of PCR products of the *rpoB* and the *embB* genes were sequenced by using respective primers that were used in PCR. For DNA sequencing of the *katG* mutation sites, alternative sequencing primers were designed, because the amplicon (1,771 bp) was much longer than other genes (Table 1). Direct sequencing of PCR products was performed with a CEQ2000 automate sequencer (Beckman Coulter, Inc., Fullerton, Calif.) and a DTCS quick-start master mix kit (Beckman Coulter, Inc.).

**Preparation of TaqMan MGB probes.** The TaqMan MGB probes were designed to hybridize with wild-type DNA by using the Primer Express program (Applied Biosystems, Foster City, Calif.). The MGB probes were synthesized by Applied Biosystems. The primers and probes used in the present study are shown in Table 1. Four of eight probes were labeled with 6-carboxyfluorescein (FAM) (emission wavelength, 518 nm) and the remaining four probes were labeled with VIC (emission wavelength, 552 nm), because these two dyes emit luminescence of different wavelengths and can be distinguished individually in one tube.

**Real-time PCR and nested PCR.** The real-time PCR mixture was prepared in a final volume of 25 μl with 12.5 μl of Universal PCR Master Mix (Applied Biosystems), 25 pmol of primer, the optimal concentration of FAM- and VIC-labeled TaqMan MGB probes (Table 1), and 5 ng of purified DNA or 1 μl of extracted DNA. Real-time PCR analysis was performed with an ABI PRISM 7700 instrument (Applied Biosystems). The conditions of PCR amplification were 50°C for 2 min, 95°C for 10 min, and then 40 cycles of 95°C for 15 s and 60°C for 1 min. Data were analyzed with Sequence Detector software (Applied Biosystems). Fluorescence of hybridized probes was expressed as ΔRn (normalized reporter signal). The number of amplification cycles required for emission of a certain luminescence intensity by each probe (ΔRn = 0.2) reflected the amount of DNA in the sample. This cycle number was called the threshold cycle (Ct). Therefore, the presence of a mutation would result in an increase in Ct.

Nested PCR was performed when signals were undetected in real-time PCR. The PCR was carried out in a 25-μl reaction volume. The reaction mixture contained 1× PCR buffer, 1 U of GC-rich enzyme mix (Roche Diagnostics Corp., Indianapolis, Ind.), a 200 μM concentration of each of the four deoxynucleoside triphosphates, a 1 μM concentration of three kinds of primer sets (Table 1), 1 M GC-rich solution, 1.5 mM $MgCl_2$, and 10 μl of template DNA. The primer pairs for the *rpoB*, *katG*, and *embB* genes amplified 534-, 464-, and 408-bp fragments, respectively. The PCR conditions were as follows: initial denaturation at 94°C for 5 min and then 40 cycles of 94°C for 30 s, 60°C for 30 s, and 72°C for 30 s. After the first PCR, the amplified product was diluted 100-fold with sterilized water. One microliter of this solution was used for the real-time PCR analysis as described above.

**IPC for detecting PCR inhibitors.** For analysis of sputum samples from TB patients, an internal process control (IPC) was performed to detect PCR inhibitors PCR simultaneously. As IPC primers, each rpoB primer was added to the 5′ end of the corresponding lambda phage primer (Table 1). The identical sequence of the lambda phage IPC-R probe, which was 5′ labeled with FAM and quenched with 6-carboxytetramethylrhodamine (TAMRA) at the 3′ end, was used for analysis as described previously (13).

**Electrophoresis.** Amplification products were separated on 3% agarose gels with 1× Tris-acetate-EDTA buffer for 45 min at 100 V.

## RESULTS

**Real-time PCR.** For rapid detection of mutations in the *rpoB*, *katG*, and *embB* genes involving *M. tuberculosis* resistance to RIF, INH, and EMB, respectively, three primer pairs and eight MGB probes were designed (Fig. 1 and Table 1). Five probes (rpo510/514, rpo514/520, rpo520/524, rpo524/529, and rpo529/533) were used for detection of mutations in the hot spot of *rpoB* (81 bp between codons 507 and 533 [equivalent to *Escherichia coli* numbering system {31}]). One probe (TB control probe) was designed outside the hot spot in *rpoB* as a control for determining the amount of DNA and for identifying *M. tuberculosis*. Polymorphisms in the 81-bp region of *rpoB* could be analyzed by using three tubes. One probe each for *embB* (codon 306) and *katG* (codon 315) was labeled with FAM and VIC, respectively. These probes were mixed with their four corresponding primers in one tube. Four tubes (three tubes for control and RIF resistance and one tube for INH and EMB resistance) were employed in the assay. Luminescence of all eight probes was detectable by real-time PCR with genomic DNA extracted from *M. tuberculosis* H37Rv as the template (Fig. 2A). When the DNA had mutations in *rpoB* at position 516 and in *katG* at position 315, the corresponding probes showed no luminescence signal (Fig. 2B). Typical results are shown in Fig. 2C and D. These results indicate that the probes used in this study can identify mutations of the target genes. Similar results were obtained by using autoclaved supernatants of *M. tuberculosis* suspensions instead of purified DNAs (data not shown).

**Specificity and sensitivity.** No luminescence was found when *M. avium* DNA (up to 50 ng) was analyzed in this system (Fig. 2E). In addition, luminescence was not detected even when more than 50 ng of DNA from other mycobacteria, such as *M. intracellulare*, *M. kansasii*, *M. marinum*, *M. simiae*, *M. asiaticum*, *M. xenopi*, *M. scrofulaceum*, *M. gordonae*, *M. malmoense*, *M. shimoidei*, *M. nonchromogenicum*, *M. fortuitum*, *M. abscessus*, *M. tokaiense*, *M. austroafricanum*, *M. pulveris*, *M. smegmatis*, and *M. leprae*, was used as the template. The presence of sufficient amounts of DNA in the system was confirmed by

TABLE 1. Designed primers and probes used in this study

| Primer or probe | Target | Conc (μM) | Sequence[a] | Product size (bp) |
|---|---|---|---|---|
| Real-time PCR | | | | |
| PCR primer | *rpoB* | 1.0 | 5′-ACACCGCAGACGTTGATCA-3′ | 363 |
| | | 1.0 | 5′-CTAGTGATGGCGGTCAGGTAC-3′ | |
| | *embB* | 1.0 | 5′-CGTGGTGATATTCGGCTTCCT-3′ | 130 |
| | | 1.0 | 5′-GCCGAACCAGCGGAAATAG-3′ | |
| | *katG* | 1.0 | 5′-TGGGCTGGAAGAGCTCGTAT-3′ | 105 |
| | | 1.0 | 5′-GGAAACTGTTGTCCCATTTCG-3′ | |
| MGB probe | TB control | 0.1 | 5′-FAM-TCTTCGGCACCAGC-MGB-3′ | |
| | rpo520/524 | 0.1 | 5′-VIC-TCAACCCCGACAGC-MGB-3′ | |
| | rpo510/514 | 0.08 | 5′-FAM-CCATGAATTGGCTCAGC-MGB-3′ | |
| | rpo514/520 | 0.06 | 5′-VIC-TTCATGGACCAGAACAA-MGB-3′ | |
| | rpo529/533 | 0.12 | 5′-FAM-CAGCGCCGACAGT-MGB-3′ | |
| | rpo524/529 | 0.04 | 5′-VIC-TGACCCACAAGCGC-MGB-3′ | |
| | emb306 | 0.08 | 5′-FAM-CTCGGGCCATGCC-MGB-3′ | |
| | kat315 | 0.04 | 5′-VIC-CACCAGCGGCATC-MGB-3′ | |
| Nested PCR | | | | |
| | *rpoB* | 1.0 | 5′-GGGAGCGGATGACCACCCA-3′ | 534 |
| | | 1.0 | 5′-TGTAGTCCACCTCAGACGAG-3′ | |
| | *embB* | 1.0 | 5′-CTGAAACTGCTGGCGATCAT-3′ | 408 |
| | | 1.0 | 5′-CAGGCGCATCCACAGACT-3′ | |
| | *katG* | 1.0 | 5′-GAGCCCGATGAGGTCTATTG-3′ | 464 |
| | | 1.0 | 5′-CTCTTCGTCAGCTCCCACTC-3′ | |
| Internal process control | | | | |
| IPC primer | *rpoB*/lambda | 1.0 | 5′-ACACCGCAGACGTTGATCA**TTTCCGGGACGTATCATGCT**-3′ | 187 |
| | | 1.0 | 5′-CTAGTGATGGCGGTCAGGTA**CACCGCTCAGGCATTTGCT**-3′ | |
| IPC probe | Lambda | 0.2 | 5′-FAM-TCCTTCGTGATATCGGACGTTGGCTG-TAMRA-3′ | |
| DNA sequencing | | | | |
| PCR and sequence | *rpoB* | 1.0, 0.2 | 5′-ACCGACGACATCGACCACTT-3′ | 528 |
| | | 1.0, 0.2 | 5′-GGCGGTCAGGTACACGATCT-3′ | |
| | *embB* | 1.0, 0.2 | 5′-CGACCACGCTGAAACTGCT-3′ | 561 |
| | | 1.0, 0.2 | 5′-CGTTGTTGAACGGCATCCAC-3′ | |
| PCR | *katG* | 1.0 | 5′-CAACCGGCTCAATCTGAAGG-3′ | 1,771 |
| | | 1.0 | 5′-CCACCTACCAGCACCGTCAT-3′ | |
| Sequence | | 0.2 | 5′-GCAGATGGGGCTGATCTACG-3′ | |
| | | 0.2 | 5′-AACTCGTCGGCCAATTCCTC-3′ | |

[a] Each TaqMan MGB probe was labeled with either FAM or VIC at the 5′ end and with both a nonfluorescent quencher and an MGB at the 3′ end. The IPC probe was labeled with FAM at the 5′ end and TAMRA at the 3′ end. The sequences of IPC primers in boldface correspond to the lambda phage DNA sequences (13).

alternative PCR with mycobacterial 16S rRNA gene primers (6) or *dnaJ* gene primers (29) (data not shown). As expected, we detected no luminescence with DNAs prepared from *K. pneumoniae*, *P. aeruginosa*, and *S. aureus*. By contrast, the other members of *M. tuberculosis* complex, such as *M. bovis*, *M. bovis* BCG, *M. africanum*, and *M. microti*, exhibited similar luminescence in the real-time PCR system (data not shown). Therefore, the specificity of this system for the *M. tuberculosis* complex was sufficiently high.

By using purified genomic DNA from *M. tuberculosis* H37Rv, the sensitivity of this system was determined. In direct real-time PCR with the *rpoB* primer set and TB control probe, 100 fg of genomic DNA could be detected. Therefore, the mutation was detectable efficiently in the presence of 250 fg (Ct = 37) of TB genomic DNA. The detection limit of the real-time PCR was 10 fg of DNA when combined with nested PCR (data not shown).

**Assessment of real-time PCR.** We extracted and sequenced genomic DNAs from 45 laboratory strains of RIF-resistant *M. tuberculosis*. They were classified into 20 groups based on their genotypes by nucleotide sequencing of *M. tuberculosis* DNAs (Table 2). The luminescence intensity of TaqMan MGB probes in the real-time PCR amplification system was expressed as Ct. The Ct was higher when mutations were present in the genes. Using 45 RIF-resistant strains, we measured the Ct derived from an internal TB control probe bound outside the hot spots of the *rpoB* gene and ΔCt, which expressed the difference between the control and each MGB probe (Table 2). It was found that the ΔCts of probes hybridizing with the region without mutations were low (from −2.44 to 1.61) and that the

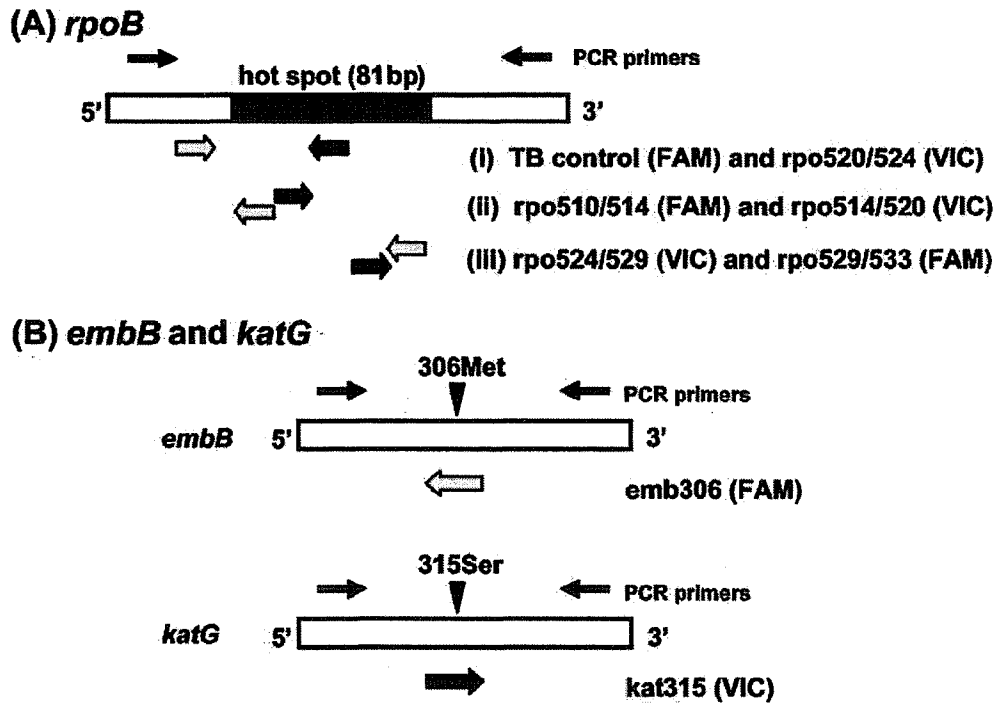


FIG. 1. Design of TaqMan MGB probes for detection of mutations in the *rpoB*, *embB*, and *katG* genes. MGB probes were labeled with two different dyes (FAM or VIC). The DNA sample and PCR primers for *rpoB* amplification were mixed with each set of probes in three different tubes: (i) TB control and rpo520/524, (ii) rpo510/514 and rpo514/520, and (iii) rpo524/529 and rpo529/533 (A). The emb306 and kat315 probes and *embB* and *katG* PCR primers were mixed and reacted in another tube (B). The sequences of primers and probes are listed in Table 1.

ΔCt was higher (≥7) when mutations existed in the target DNA that should hybridize with the MGB probe. These results suggest that a ΔCt of more than 7 was associated with a mutation in the nucleotide sequence. No strains that had mutations within the codons 510 to 514 of the *rpoB* gene were found. To check to the specificity of the rpo510/514 probe, the *rpoB* gene was cloned and mutations were constructed at codons 511 (CTG→CCG) and 513 (CAA→CTA). Real-time

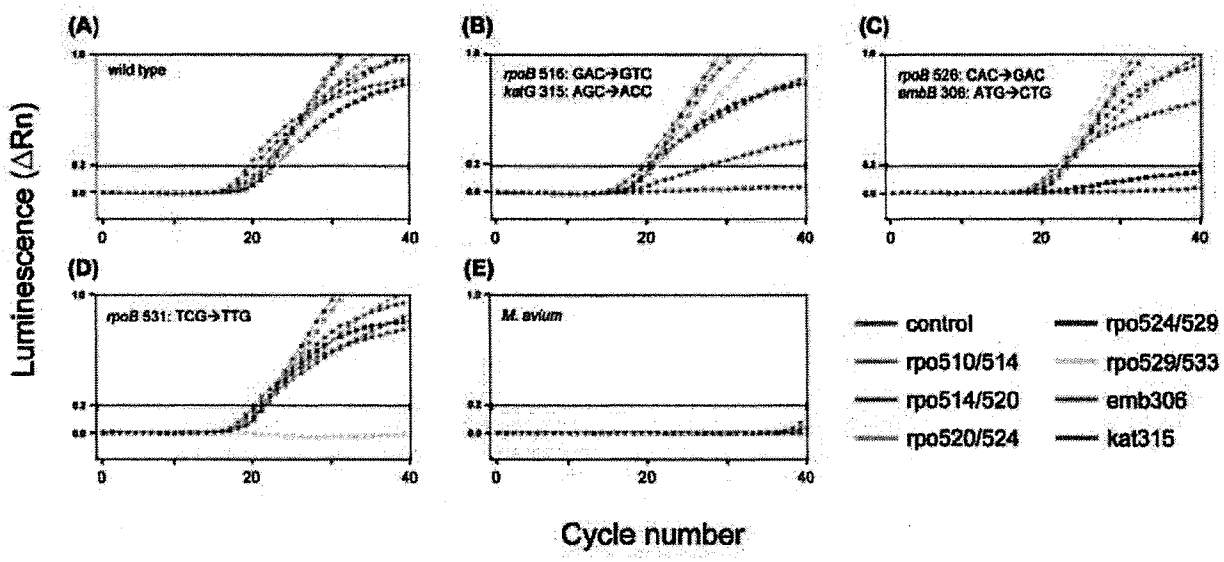


FIG. 2. Analysis of DNAs from mycobacteria with eight TaqMan MGB probes by real-time PCR. The templates were genomic DNAs extracted from *M. tuberculosis* H37Rv (A) as a control, certain mutants of *M. tuberculosis* (B, *rpoB* and *katG*; C, *rpoB* and *embB*; and D, *rpoB*), and *M. avium* (E). The *x* axis shows cycle numbers of PCR, and the *y* axis represents the normalized reporter signal (ΔRn). A horizontal line indicates the threshold (ΔRn = 0.2). The Ct is expressed as the number of cycles to reach the threshold.

TABLE 2. Luminescent patterns of real-time PCR with DNAs from 45 laboratory strains of RIF-resistant *M. tuberculosis*[a]

| Mutant position[b] | No. of strains | Control Ct[c] (mean ± SD) | ΔCt[d] (mean ± SD) | | | | | | |
|---|---|---|---|---|---|---|---|---|---|
| | | | rpo510/514 | rpo514/519 | rpo520/524 | rpo524/529 | rpo529/533 | emb306 | kat315 |
| wt[e] | 7 | 21.33 ± 0.89 | 0.19 ± 1.22 | −0.48 ± 0.82 | −0.42 ± 0.15 | 0.65 ± 0.68 | 1.11 ± 0.85 | −0.82 ± 1.22 | −1.69 ± 0.98 |
| *rpoB* 516, GAC→GTC | 1 | 20.67 | −0.25 | **8.11** | 0.02 | 1.14 | 1.61 | 0.31 | −0.45 |
| *rpoB* 516, GAC→GTC<br>*katG* 315, AGC→ACC | 7 | 21.43 ± 1.38 | 0.89 ± 0.49 | **7.19 ± 0.33** | −0.27 ± 0.27 | 0.84 ± 0.38 | 1.09 ± 0.55 | −1.05 ± 0.40 | **>17.19** |
| *rpoB* 516, GAC→GTC<br>*rpoB* 522, TCG→TTG<br>*katG* 315, AGC→ACC | 1 | 22.18 | −0.57 | **>17.82** | **12.96** | 0.79 | 0.94 | −1.08 | **>17.82** |
| *rpoB* 520, CCG→TCG<br>*rpoB* 522, TCG→TTG | 1 | 20.53 | 0.64 | −0.35 | **14.47** | 0.64 | 0.85 | −0.89 | −1.74 |
| *rpoB* 520, CCG→TCG<br>*rpoB* 522, TCG→TTG<br>*katG* 315, AGC→ACC | 1 | 22.29 | 0.25 | −0.34 | **16.06** | 0.46 | 0.76 | −1.62 | **>17.71** |
| *rpoB* 522, TCG→TTG | 1 | 22.36 | −0.37 | −0.43 | **15.58** | 0.37 | 0.54 | −1.78 | −2.44 |
| *rpoB* 526, CAC→TAC<br>*katG* 315, AGC→ACC | 1 | 23.20 | −0.55 | −0.70 | −0.43 | **>16.80** | −0.21 | −1.25 | **>16.80** |
| *rpoB* 526, CAC→CGC<br>*katG* 315, AGC→ACC | 1 | 19.33 | 0.02 | −1.04 | −0.24 | **>20.67** | −0.36 | −1.16 | **>20.67** |
| *rpoB* 526, CAC→CGC<br>*embB* 306, ATG→ATA | 1 | 22.87 | −1.11 | −0.59 | −0.29 | **>17.13** | −0.51 | **>17.13** | −2.12 |
| *rpoB* 526, CAC→GAC<br>*embB* 306, ATG→CTG | 1 | 23.09 | −0.49 | −0.37 | −0.60 | **>16.91** | −1.24 | **>16.91** | −1.25 |
| *rpoB* 526, CAC→AGC<br>*embB* 306, ATG→GTG<br>*katG* 315, AGC→ACC | 1 | 23.44 | −1.14 | −0.54 | −0.40 | **>16.56** | −0.40 | **>16.56** | **>16.56** |
| *rpoB* 531, TCG→TTG | 11 | 21.73 ± 1.77 | 0.22 ± 1.18 | −0.28 ± 0.33 | −0.31 ± 1.88 | 0.05 ± 0.32 | **>16.50** | −0.84 ± 1.12 | −1.55 ± 1.34 |
| *rpoB* 531, TCG→TGG | 1 | 19.10 | 1.00 | 0.47 | −0.28 | 0.78 | **20.90** | 0.23 | −0.53 |
| *rpoB* 531, TCG→TTG<br>*katG* 315, AGC→ACC | 2 | 20.89 ± 0.76 | 0.20 ± 0.59 | −0.33 ± 0.33 | 0.07 ± 0.10 | 0.11 ± 0.32 | **>18.36** | −0.96 ± 0.42 | **>18.36** |
| *rpoB* 531, TCG→TTG<br>*embB* 306, ATG→ATC | 2 | 21.77 ± 1.16 | 0.86 ± 0.24 | −0.04 ± 0.11 | −0.33 ± 0.14 | 0.37 ± 0.20 | **>17.07** | **>17.07** | −0.78 ± 0.16 |
| *rpoB* 531, TCG→TTG<br>*embB* 306, ATG→GTG | 3 | 20.90 ± 0.47 | 0.63 ± 0.65 | −0.02 ± 0.23 | −0.24 ± 0.17 | 0.35 ± 0.30 | **>18.63** | **>18.63** | −0.78 ± 0.70 |
| *rpoB* 531, TCG→TTG<br>*embB* 306, ATG→CTG | 1 | 20.78 | −0.28 | −0.07 | −0.22 | 0.48 | **>18.22** | **>18.22** | −1.87 |
| *rpoB* 531, TCG→TTG<br>*embB* 306, ATG→ATC<br>*katG* 315, AGC→ACC | 5 | 22.04 ± 1.52 | −0.01 ± 0.35 | −0.30 ± 0.28 | −0.21 ± 0.27 | 0.00 ± 0.12 | **>16.44** | **>16.44** | **>16.44** |
| *rpoB* 531, TCG→TGG<br>*embB* 306, ATG→GTG<br>*katG* 315, AGC→ACC | 1 | 22.24 | −1.03 | −0.52 | −0.08 | −0.04 | **>17.76** | **>17.76** | **>17.76** |
| *rpoB* 531, TCG→TGG<br>*embB* 306, ATG→ATC<br>*katG* 315, AGC→ACC | 2 | 21.20 ± 0.16 | 0.40 ± 0.11 | −0.45 ± 0.03 | 0.05 ± 0.06 | −0.17 ± 0.15 | **>18.64** | **>18.64** | **>18.64** |

[a] Forty-five laboratory strains of RIF-resistant *M. tuberculosis*, including MDR *M. tuberculosis*.
[b] Gene, codon number, and allele of the mutation(s) in the strain.
[c] Cycle number required when luminescence of control probe reaches the threshold (ΔRn = 0.2).
[d] Difference in Ct between control probe and corresponding probe. The mutations resulted in an increased ΔCt, which is indicated by boldface.
[e] Wild-type, pansusceptible strains, including *M. tuberculosis* H37Rv.

TABLE 3. Luminescence patterns of real-time PCR with DNA extracted from sputua of TB patients[a]

| Sample | Smear | Culture | Resistance phenotype | Mutant position[b] | Control Ct[c] | ΔCt[d] | | | | | | |
|---|---|---|---|---|---|---|---|---|---|---|---|---|
| | | | | | | rpo510/514 | rpo514/519 | rpo520/524 | rpo524/529 | rpo529/533 | emb306 | kat315 |
| C1 | − | + | − | − | >40.00 | ND[e] | ND | ND | ND | ND | ND | ND |
| Nested PCR | | | | | 18.91 | 0.38 | 0.77 | −0.11 | 1.57 | 1.34 | −1.44 | −0.36 |
| C2 | + | + | − | − | 34.07 | −0.12 | −1.10 | 0.06 | 2.46 | 2.05 | −3.30 | −2.47 |
| C3 | − | + | − | − | 27.95 | −1.99 | −2.85 | −0.22 | −0.63 | −1.47 | −1.86 | −0.77 |
| C4 | − | + | − | − | >40.00 | ND | ND | ND | ND | ND | ND | ND |
| Nested PCR | | | | | 17.00 | 1.38 | 0.55 | 1.55 | 1.40 | 0.03 | 0.55 | 0.62 |
| C5 | − | + | INH | *katG* 315, AGC→ACC | 33.11 | 3.15 | 2.49 | 0.20 | 0.85 | 0.24 | −3.28 | **>6.79** |
| C6 | − | + | − | − | 37.31 | 0.65 | 0.29 | 0.02 | 1.65 | 1.77 | −3.35 | −3.07 |
| C7 | − | + | − | − | >40.00 | ND | ND | ND | ND | ND | ND | ND |
| Nested PCR | | | | | 20.06 | 0.38 | 0.90 | −0.24 | 1.31 | 1.20 | −0.55 | −0.87 |
| C8 | + | + | − | − | 31.70 | 0.92 | 0.82 | 0.82 | 2.79 | 2.40 | −0.79 | −0.37 |
| C9 | + | + | − | − | 39.39 | ND | ND | ND | ND | ND | ND | ND |
| Nested PCR | | | | | 15.23 | 2.01 | 2.13 | −0.04 | 2.01 | 1.40 | −0.69 | −1.39 |
| C10 | + | + | − | − | 36.35 | −2.12 | −1.36 | −0.08 | −0.26 | 0.06 | −2.52 | −3.40 |
| C11 | − | + | RIF, INH, EMB | *rpoB* 531, TCG→TTG; *katG* 315, AGC→ACC; *embB* 306, ATG→GTG | 31.08 | 0.50 | 0.04 | 0.01 | 0.14 | **>8.92** | **>8.92** | **>8.92** |
| C12 | − | + | − | − | 34.70 | −0.15 | 0.18 | 0.59 | 1.51 | 1.81 | −3.36 | −2.60 |
| C13 | − | + | − | − | >40.00 | ND | ND | ND | ND | ND | ND | ND |
| Nested PCR | | | | | 19.11 | 0.64 | −0.37 | −0.12 | 0.87 | 1.35 | 1.36 | −1.06 |
| C14 | − | + | − | − | >40.00 | ND | ND | ND | ND | ND | ND | ND |
| Nested PCR | | | | | 21.80 | 0.45 | −0.45 | −0.11 | 0.94 | 1.17 | −1.52 | 0.67 |
| C15 | − | + | − | − | 13.94 | 1.35 | 0.43 | −0.26 | 0.93 | 1.42 | 0.75 | 0.05 |
| C16 | − | + | − | − | >40.00 | ND | ND | ND | ND | ND | ND | ND |
| Nested PCR | | | | | 19.96 | 0.69 | −0.10 | −0.09 | 1.04 | 1.03 | −1.65 | −1.39 |
| C17 | − | + | − | − | 31.73 | 1.12 | 1.12 | −0.06 | 2.34 | 2.16 | −2.37 | −0.77 |
| C18 | − | + | − | − | 33.19 | 1.04 | 0.26 | 0.42 | 1.81 | 1.36 | −2.72 | −1.94 |
| C19 | − | + | − | − | 36.23 | −2.22 | 0.42 | −0.04 | 1.90 | 2.28 | −2.69 | −2.07 |
| C20 | + | − | ND | − | >40.00 | ND | ND | ND | ND | ND | ND | ND |
| Nested PCR | | | | | 21.28 | 0.62 | −0.27 | 0.00 | 1.24 | 1.70 | −0.72 | −2.33 |
| C21 | − | + | − | − | 35.52 | 0.60 | −0.47 | 0.15 | 1.19 | 1.37 | −3.24 | −2.49 |
| C22 | + | + | − | − | >40.00 | ND | ND | ND | ND | ND | ND | ND |
| Nested PCR | | | | | 19.93 | 0.23 | −0.58 | −0.13 | 0.66 | 0.93 | −0.93 | −2.15 |
| C23 | − | − | ND | − | >40.00 | ND | ND | ND | ND | ND | ND | ND |
| Nested PCR | | | | | 15.71 | −0.08 | −0.92 | −0.19 | 0.13 | −0.15 | −0.72 | −2.33 |
| C24 | − | + | − | − | 36.45 | 0.92 | 0.05 | 0.81 | 1.97 | 1.72 | −3.04 | −2.23 |
| C25 | − | + | − | − | 32.70 | 2.16 | 2.57 | 0.21 | 1.96 | 1.36 | −3.04 | −1.95 |
| C26 | + | + | − | − | 36.40 | 0.10 | 0.20 | 0.21 | 2.00 | 2.02 | −3.33 | −2.61 |
| C27 | + | + | − | − | >40.00 | ND | ND | ND | ND | ND | ND | ND |
| Nested PCR | | | | | 18.68 | 1.68 | 0.64 | 0.12 | 1.30 | 2.37 | 1.29 | 1.11 |

[a] DNAs derived from *M. tuberculosis* were detected with the COBAS AMPLICOR PCR system.
[b] Gene, codon number, and allele of mutations in *M. tuberculosis* DNA extracted from sputa of TB patients.
[c] Cycle number required when luminescence of control probe reaches the threshold (ΔRn = 0.2).
[d] Difference in Ct between control probe and corresponding probe. The mutations resulted in an increased ΔCt, which is indicated by boldface.
[e] ND, not detected.

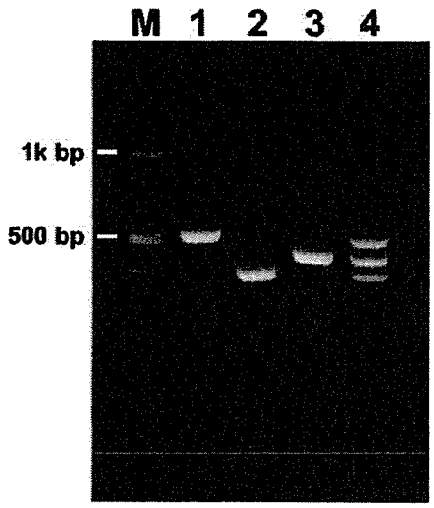


FIG. 3. DNA analysis of amplicons by simplex and multiplex PCRs. DNA from sputum sample C1 was amplified by using primers for the *rpoB*, *embB*, and *katG* genes. The product sizes of their amplicons were 534, 408, and 464 bp, respectively (lanes 1 to 3, respectively). Three kinds of primer sets for the *rpoB*, *embB*, and *katG* genes were mixed, and multiplex PCR was performed (lane 4). The M lane was a DNA molecular size marker which contained the 100-bp ladder.

PCR analysis with each construct as the template showed that the luminescence that was derived from probe rpo510/514 disappeared completely (data not shown).

**Clinical application of real-time PCR.** DNAs extracted from sputa of patients with pulmonary TB were examined to assess to possibility of rapid detection of drug-resistant *M. tuberculosis* in clinical specimens by real-time PCR. Twenty-five clinical samples were culture positive, and two samples were culture negative. Nine samples were smear positive, and 18 samples were negative (Table 3). Real-time PCR was used to analyze sputum samples for detection of mutations. Sample C5 had a mutation at codon 315 in the *katG* gene, and sample C11 possessed mutations at codon 531 in the *rpoB* gene, codon 315 in the *katG* gene, and codon 306 in the *embB* gene. These findings were in agreement with the results obtained by DNA sequencing. The drug susceptibility phenotypes of clinical isolates assessed by conventional culture methods were consistent with the genotypes (Table 3). Thus, our real-time PCR system can detect mutations even when clinical samples, such as sputa, are used.

A total of 16 of 27 sputum samples (59.3%) showed strong luminescence in real-time PCR. By contrast, 11 samples showed no luminescence even after 40 cycles of PCR amplification. This was probably due to low concentrations, because IPC was positive for all 11 samples. Consequently, we performed site-specific nested PCR when the amount of DNA was small. The *rpoB*, *katG*, and *embB* genes were amplified by PCR with their corresponding primer sets (Fig. 3). By optimizing the PCR conditions with six primers, three fragments that contained the target sites at a similar concentration were amplified (Fig. 3, lane 4). The targets (*rpoB*, *katG*, and *embB*) were amplified by nested PCR with one tube. The targets were then analyzed by using real-time PCR. Nested PCR products could be analyzed for the presence of mutations associated with drug resistance, although DNA was undetectable in a single-step real-time PCR in these 11 samples. When nested PCR was used before real-time PCR, analysis of all 27 samples could be performed appropriately (Table 4). However, in analysis of clinical samples, the Ct was more variable, resulting in a larger ΔCt (from −3.40 to 3.15) than for purified DNAs extracted from laboratory strains (from −2.44 to 1.61).

## DISCUSSION

The TaqMan MGB probes are currently used for detection of single-nucleotide polymorphisms, because they can distinguish one-base mismatches (1, 12, 18). In the present study, we have attempted to apply these probes to detect drug resistance on a genetic basis. The implication of all studies on the genetic basis of antimicrobial resistance in *M. tuberculosis* is that the MDR phenotype (defined as simultaneous resistance to at least INH and RIF) is the result of accumulative mutations (10, 23). The major anti-TB drugs are INH, RIF, and EMB. Among them, INH and RIF are the most potent agents. More than 90% of RIF-resistant *M. tuberculosis* isolates possess a point mutation at the hot spot in the 81-bp region of *rpoB* (3, 26). For that reason, detection of mutations in the *rpoB* gene is a quite useful strategy for diagnosis.

The present study also analyzed extracted DNAs from *M. tuberculosis* by real-time PCR for the presence of mutations in the *katG* (codon 315) and *embB* (codon 306) genes. Codons 315 in *katG* and 306 in *embB* were selected because mutations at these sites have been observed frequently in INH- and EMB-resistant *M. tuberculosis* (3, 4, 11, 28). However, the role of codon 306 in the *embB* gene for EMB resistance remains controversial, because the mutation has also been found in EMB-susceptible *M. tuberculosis*. It has been reported that *embB*306 mutations were detected in 48% of EMB-resistant strains and in 31% of EMB-susceptible strains (21). In particular, 60% of EMB-susceptible strains were resistant to rifampin and isoniazid (i.e., MDR), but none of pansusceptible strains harbored an *embB*306 mutation. A discrepancy between the results of phenotypic and genotypic analyses of EMB resistance tests was restricted to the strains that were already resistant to other anti-TB drugs, such as MDR *M. tuberculosis*. Our results have shown that 42% of EMB-susceptible strains of MDR *M. tuberculosis* had the mutation, in contrast to 0% of pansusceptible strains. When a mutation exists at *embB*306 in MDR *M. tuberculosis*, it is possible that the strain is susceptible to EMB. Nevertheless, 70% of EMB-resistant strains have a point mutation at codon 306 in the *embB* gene (3, 28). The mutation of codon 315 (Ser) in the *katG* gene is the most frequently encountered mutation that is associated with INH resistance (30 to 65%) (4, 11). In the present study, we found that 70% of INH-resistant strains and 6% of INH-susceptible strains had the mutation at this site. These results are consistent with previous reports (4, 11, 21).

The results obtained from the real-time PCR system in this study were consistent with DNA sequencing analyses of 45 laboratory strains and 27 clinical samples. The system did not react with DNAs prepared from *K. pneumoniae*, *P. aeruginosa*, *S. aureus*, and nontuberculous mycobacteria but reacted solely with DNAs from isolates belonging to the *M. tuberculosis* com-

TABLE 4. Detection of genotypes by real-time PCR

| Sample type and analysis | No. of samples | No. (%) detected | No. (%) undetected |
|---|---|---|---|
| DNAs from cultured bacilli | 45 | 45 (100) | 0 (0) |
| DNAs from sputa of TB patients[a] | | | |
| Direct analysis | 27 | 16 (59.3) | 11 (40.7) |
| Preamplified DNA (after nested PCR)[b] | 11 | 11 (100) | 0 (0) |

[a] DNAs were extracted from sputa of TB patients by use of the AMPLICOR respiratory specimen preparation kit.
[b] DNAs from sputa were analyzed after preamplification by nested PCR.

plex. These results imply that the primers and probes used here are specific for *M. tuberculosis* complex.

Although understanding the mechanisms of drug resistance has practical implications for rapid detection of drug-resistant TB by molecular methods, there are a number of limitations to widespread use of PCR-based techniques. For one, resistance to anti-TB agents involves changes in multiple genes and at multiple possible locations within a gene. This fact complicates testing for the various genes. In addition, not all possible genes or mechanisms of resistance have been identified, which represents a significant drawback for diagnostics.

It has been reported previously that real-time PCR with MGB probes was applied for detection of INH-resistant *M. tuberculosis* (34). In that study, DNAs prepared from smear-positive sputa were used. However, the results for certain samples were inconsistent with those of DNA sequencing. One possible explanation for this is that the amount and/or quality of DNA was not standardized in the study (34). Our results suggest that the amount of DNA in the sample is critical for analysis with real-time PCR using TaqMan MGB probes. The quality of DNA (e.g., whether it is inhibitor free) is also important. In the present study, two control probes were designed for the real-time PCR. One was a TB control probe for identification of *M. tuberculosis* and confirmation of DNA amount; the other was the IPC for detection of PCR inhibitors. If luminescence is not detected, the reason mentioned above can be suspected.

Several molecular methods to detect drug-resistant *M. tuberculosis* have been reported (8). These methods are fundamentally based on the detection of point mutations. PCR-DNA sequencing is a straightforward technology to detect mutation (14), although it takes 1 to 2 days until the result is obtained. Methods based on real-time PCR have utilized fluorescence resonance energy transfer (FRET) probes (9, 32), molecular beacons (6, 23, 24), and TaqMan MGB probes (34). By using the real-time PCR as described here, the time to obtain results for drug susceptibility or resistance can be shortened to as little as 3 h from the preparation of DNAs from isolates of *M. tuberculosis* and sputum samples. Rapid detection of drug resistance or susceptibility may open new therapeutic avenues for intervention in diseases in which drug resistance is a major impediment to treatment. The method based on FRET probes requires a longer probe, because it utilizes both sensor and anchor probes (33). The shift of melting temperature was unclear in some cases when long probes were used in FRET analysis to detect mutations. By contrast, molecular beacons and TaqMan MGB probes, which can be designed to be shorter than FRET probe, detect the mutations on the basis of either emission or lack of emission of luminescence. The luminescence can be measured with a fluorescence plate reader after conventional PCR, even without a real-time PCR analyzer (5).

Molecular beacons are an alternative approach to detect drug-resistant organisms in a real-time format. It has been reported that RIF-resistant *M. tuberculosis* can be detected in a one-tube reaction by using the beacons (6). This is a convenient and simple method to detect mutations. However, it is necessary to use a real-time PCR analyzer that can detect five kinds of different luminescence simultaneously. Although the assay described here requires the use of four tubes per sample, only two wavelengths are employed, enabling the use of less advanced equipment.

Our present study suggests that drug-resistant *M. tuberculosis* can be detected by ΔCt with TaqMan MGB probes in real-time PCR. Based on the result for 45 laboratory strains and 27 clinical samples of *M. tuberculosis*, ΔCt was less than 3.5 when organisms had no mutation (Tables 2 and 3). When ΔCt was more than 6, the DNA samples contained mutations within the target region. These isolates or samples are strongly inferred to be drug-resistant *M. tuberculosis* (Tables 2 and 3). When wild-type and mutated DNAs were mixed at ratios ranging from 8:2 to 2:8, ΔCt was distributed between 3.5 and 6.0 (data not shown). Indeed, ΔCt of a mixture of drug-susceptible and -resistant bacilli ranged from 3.5 to 6.0. When ΔCt is distributed within the range of 3.5 to 6.0, DNA sequencing analysis should be performed to confirm the mixture. In analysis of clinical samples without mutations, the range of ΔCt became larger (−3.40 to 3.15) than that of purified DNAs extracted from laboratory strains (−2.44 to 1.61). It is thought that ΔCt obtained from the real-time PCR is a useful marker for discriminating between drug-susceptible and drug-resistant *M. tuberculosis* strains. These criteria are applicable to detect drug-resistant *M. tuberculosis* in clinical laboratories.

Real-time-based PCR shows sufficient specificity and sensitivity to detect drug-resistant *M. tuberculosis* even with sputum samples from TB patients without culture. The real-time PCR described here can detect drug-resistant *M. tuberculosis* within 3 h from DNA preparation. For those reasons, it may be a powerful tool for control of drug-resistant *M. tuberculosis*.

## ACKNOWLEDGMENTS

This work was supported by grants from the Ministry of Health, Labour and Welfare (Research on Emerging and Re-emerging Infectious Diseases, Health Sciences Research Grants); the Ministry of Education, Culture, Sports, Science and Technology; the Ministry of the Environment (Global Environment Research Fund); Osaka City University (Urban Research Project); and the United States-Japan Cooperative Medical Science Program against Tuberculosis and Leprosy.

## REFERENCES

1. **An, P., G. W. Nelson, L. Wang, S. Donfield, J. J. Goedert, J. Phair, D. Vlahov, S. Buchbinder, W. L. Farrar, W. Modi, S. J. O'Brien, and C. A. Winkler.** 2002. Modulating influence on HIV/AIDS by interacting RANTES gene variants. Proc. Natl. Acad. Sci. USA **99**:10002–10007.
2. **Bloom, B. R.** 2002. Tuberculosis—the global view. N. Engl. J. Med. **346**: 1434–1435.
3. **Cockerill, F. R., III.** 1999. Genetic methods for assessing antimicrobial resistance. Antimicrob. Agents Chemother. **43**:199–212.

4. **Cockerill, F. R., III, J. R. Uhl, Z. Temesgen, Y. Zhang, L. Stockman, G. D. Roberts, D. L. Williams, and B. C. Kline.** 1995. Rapid identification of a point mutation of the *Mycobacterium tuberculosis* catalase-peroxidase (*katG*) gene associated with isoniazid resistance. J. Infect. Dis. **171**:240–245.
5. **de Kok, J. B., E. T. Wiegerinck, B. A. Giesendorf, and D. W. Swinkels.** 2002. Rapid genotyping of single nucleotide polymorphisms using novel minor groove binding DNA oligonucleotides (MGB probes). Hum. Mutat. **19**:554–559.
6. **El-Hajj, H. H., S. A. Marras, S. Tyagi, F. R. Kramer, and D. Alland.** 2001. Detection of rifampin resistance in *Mycobacterium tuberculosis* in a single tube with molecular beacons. J. Clin. Microbiol. **39**:4131–4137.
7. **Espinal, M. A., A. Laszlo, L. Simonsen, F. Boulahbal, S. J. Kim, A. Reniero, S. Hoffner, H. L. Rieder, N. Binkin, C. Dye, R. Williams, M. C. Raviglione, et al.** 2001. Global trends in resistance to antituberculosis drugs. N. Engl. J. Med. **344**:1294–1303.
8. **Garcia de Viedma, D.** 2003. Rapid detection of resistance in *Mycobacterium tuberculosis*: a review discussing molecular approaches. Clin. Microbiol. Infect. **9**:349–359.
9. **Garcia de Viedma, D., M. del Sol Diaz Infantes, F. Lasala, F. Chaves, L. Alcala, and E. Bouza.** 2002. New real-time PCR able to detect in a single tube multiple rifampin resistance mutations and high-level isoniazid resistance mutations in *Mycobacterium tuberculosis*. J. Clin. Microbiol. **40**:988–995.
10. **Gillespie, S. H.** 2002. Evolution of drug resistance in *Mycobacterium tuberculosis*: clinical and molecular perspective. Antimicrob. Agents Chemother. **46**:267–274.
11. **Heym, B., P. M. Alzari, N. Honore, and S. T. Cole.** 1995. Missense mutations in the catalase-peroxidase gene, katG, are associated with isoniazid resistance in *Mycobacterium tuberculosis*. Mol. Microbiol. **15**:235–245.
12. **Holloway, J. W., B. Beghe, S. Turner, L. J. Hinks, I. N. Day, and W. M. Howell.** 1999. Comparison of three methods for single nucleotide polymorphism typing for DNA bank studies: sequence-specific oligonucleotide probe hybridisation, TaqMan liquid phase hybridisation, and microplate array diagonal gel electrophoresis (MADGE). Hum. Mutat. **14**:340–347.
13. **Jensen, J. S., E. Bjornelius, B. Dohn, and P. Lidbrink.** 2004. Use of TaqMan 5′ nuclease real-time PCR for quantitative detection of *Mycoplasma genitalium* DNA in males with and without urethritis who were attendees at a sexually transmitted disease clinic. J. Clin. Microbiol. **42**:683–692.
14. **Kapur, V., L. L. Li, S. Iordanescu, M. R. Hamrick, A. Wanger, B. N. Kreiswirth, and J. M. Musser.** 1994. Characterization by automated DNA sequencing of mutations in the gene (*rpoB*) encoding the RNA polymerase beta subunit in rifampin-resistant *Mycobacterium tuberculosis* strains from New York City and Texas. J. Clin. Microbiol. **32**:1095–1098.
15. **Kent, P. R., and G. P. Kubica.** 1985. Public health mycobacteriology: a guide for the level III laboratory. U.S. Department of Health and Human Services, Washington, D.C.
16. **Kozak, M.** 1987. An analysis of 5′-noncoding sequences from 699 vertebrate messenger RNAs. Nucleic Acids Res. **15**:8125–8148.
17. **Kubica, G. P., W. E. Dye, M. L. Cohn, and G. Middlebrook.** 1963. Sputum digestion and decontamination with N-acetyl-L-cysteine-sodium hydroxide for culture of mycobacteria. Am. Rev. Respir. Dis. **87**:775–779.
18. **Kutyavin, I. V., I. A. Afonina, A. Mills, V. V. Gorn, E. A. Lukhtanov, E. S. Belousov, M. J. Singer, D. K. Walburger, S. G. Lokhov, A. A. Gall, R. Dempcy, M. W. Reed, R. B. Meyer, and J. Hedgpeth.** 2000. 3′-Minor groove binder-DNA probes increase sequence specificity at PCR extension temperatures. Nucleic Acids Res. **28**:655–661.
19. **Maeda, S., M. Matsuoka, N. Nakata, M. Kai, Y. Maeda, K. Hashimoto, H. Kimura, K. Kobayashi, and Y. Kashiwabara.** 2001. Multidrug resistant *Mycobacterium leprae* from patients with leprosy. Antimicrob. Agents Chemother. **45**:3635–3639.
20. **Martin-Casabona, N., D. Xairo Mimo, T. Gonzalez, J. Rossello, and L. Arcalis.** 1997. Rapid method for testing susceptibility of *Mycobacterium tuberculosis* by using DNA probes. J. Clin. Microbiol. **35**:2521–2525.
21. **Mokrousov, I., T. Otten, B. Vyshnevskiy, and O. Narvskaya.** 2002. Detection of *embB306* mutations in ethambutol-susceptible clinical isolates of *Mycobacterium tuberculosis* from northwestern Russia: implications for genotypic resistance testing. J. Clin. Microbiol. **40**:3810–3813.
22. **Morris, S., G. H. Bai, P. Suffys, L. Portillo-Gomez, M. Fairchok, D. Rouse, A. Telenti, N. Honore, C. Bernasconi, J. March, A. Ortega, B. Heym, H. E. Takiff, and S. T. Cole.** 1995. Molecular mechanisms of multiple drug resistance in clinical isolates of *Mycobacterium tuberculosis*. J. Infect. Dis. **171**: 954–960.
23. **Piatek, A. S., A. Telenti, M. R. Murray, H. El-Hajj, W. R. Jacobs, Jr., F. R. Kramer, and D. Alland.** 2000. Genotypic analysis of *Mycobacterium tuberculosis* in two distinct populations using molecular beacons: implications for rapid susceptibility testing. Antimicrob. Agents Chemother. **44**:103–110.
24. **Piatek, A. S., S. Tyagi, A. C. Pol, A. Telenti, L. P. Miller, F. R. Kramer, and D. Alland.** 1998. Molecular beacon sequence analysis for detecting drug resistance in *Mycobacterium tuberculosis*. Nat. Biotechnol. **16**:359–363.
25. **Rajalahti, I., P. Vuorinen, M.-M. Nieminen, and A. Miettinen.** 1998. Detection of *Mycobacterium tuberculosis* complex in sputum specimens by the automated Roche Cobas Amplicor Mycobacterium Tuberculosis Test. J. Clin. Microbiol. **36**:975–978.
26. **Ramaswamy, S., and J. M. Musser.** 1998. Molecular genetic basis of antimicrobial agent resistance in *Mycobacterium tuberculosis*: 1998 update. Tuber. Lung Dis. **79**:3–29.
27. **Sreevatsan, S., X. Pan, Y. Zhang, V. Deretic, and J. M. Musser.** 1997. Analysis of the *oxyR-ahpC* region in isoniazid-resistant and -susceptible *Mycobacterium tuberculosis* complex organisms recovered from diseased humans and animals in diverse localities. Antimicrob. Agents Chemother. **41**: 600–606.
28. **Sreevatsan, S., K. E. Stockbauer, X. Pan, B. N. Kreiswirth, S. L. Moghazeh, W. R. Jacobs, Jr., A. Telenti, and J. M. Musser.** 1997. Ethambutol resistance in *Mycobacterium tuberculosis*: critical role of *embB* mutations. Antimicrob. Agents Chemother. **41**:1677–1681.
29. **Takewaki, S., K. Okuzumi, H. Ishiko, K. Nakahara, A. Ohkubo, and R. Nagai.** 1993. Genus-specific polymerase chain reaction for the mycobacterial *dnaJ* gene and species-specific oligonucleotide probes. J. Clin. Microbiol. **31**:446–450.
30. **Telenti, A., N. Honore, C. Bernasconi, J. March, A. Ortega, B. Heym, H. E. Takiff, and S. T. Cole.** 1997. Genotypic assessment of isoniazid and rifampin resistance in *Mycobacterium tuberculosis*: a blind study at reference laboratory level. J. Clin. Microbiol. **35**:719–723.
31. **Telenti, A., P. Imboden, F. Marchesi, D. Lowrie, S. Cole, M. J. Colston, L. Matter, K. Schopfer, and T. Bodmer.** 1993. Detection of rifampicin-resistance mutations in *Mycobacterium tuberculosis*. Lancet **341**:647–650.
32. **Torres, M. J., A. Criado, J. C. Palomares, and J. Aznar.** 2000. Use of real-time PCR and fluorimetry for rapid detection of rifampin and isoniazid resistance-associated mutations in *Mycobacterium tuberculosis*. J. Clin. Microbiol. **38**:3194–3199.
33. **Torres, M. J., A. Criado, M. Ruiz, A. C. Llanos, J. C. Palomares, and J. Aznar.** 2003. Improved real-time PCR for rapid detection of rifampin and isoniazid resistance in *Mycobacterium tuberculosis* clinical isolates. Diagn. Microbiol. Infect. Dis. **45**:207–212.
34. **van Doorn, H. R., E. C. Claas, K. E. Templeton, A. G. van der Zanden, A. te Koppele Vije, M. D. de Jong, J. Dankert, and E. J. Kuijper.** 2003. Detection of a point mutation associated with high-level isoniazid resistance in *Mycobacterium tuberculosis* by using real-time PCR technology with 3′-minor groove binder-DNA probes. J. Clin. Microbiol. **41**:4630–4635.
35. **World Health Organization.** 1977. Guidelines for surveillance of drug resistance in tuberculosis. Publication no. W.H.O./TB/96.216 World Health Organization, Geneva, Switzerland.
36. **World Health Organization.** 2003. W.H.O. report 2003 global tuberculosis control. http://www.who.int/gtb/publications/globrep/index.html.

THE JOURNAL OF BIOLOGICAL CHEMISTRY Vol. 279, No. 38, Issue of September 17, pp. 39798–39806, 2004
*Printed in U.S.A.*

# Extracellular Mycobacterial DNA-binding Protein 1 Participates in *Mycobacterium*-Lung Epithelial Cell Interaction through Hyaluronic Acid*

Received for publication, March 9, 2004, and in revised form, June 3, 2004
Published, JBC Papers in Press, July 2, 2004, DOI 10.1074/jbc.M402677200

**Keiko Aoki‡, Sohkichi Matsumoto‡§, Yukio Hirayama‡, Takayuki Wada‡¶, Yuriko Ozeki‡‖, Makoto Niki‡, Pilar Domenech**, Kiyoko Umemori‡‡, Saburo Yamamoto‡‡, Amao Mineda§§, Makoto Matsumoto¶¶, and Kazuo Kobayashi‡**

*From the ‡Department of Host Defense, Osaka City University Graduate School of Medicine, 1-4-3 Asahi-machi, Abeno-ku, Osaka 545-8585, Japan, the ¶Osaka City Institute of Public Health and Environmental Sciences, Osaka 545-8585, Japan, ‖Osaka International College for Woman, 6-21-57 Tohdacho, Moriguchi, Osaka 570-8555, Japan, the **Tuberculosis Research Section, Laboratory of Immunogenetics, NIAID, National Institutes of Health, Rockville, Maryland 20852, the ‡‡Department of Bacterial and Blood Products, National Institute of Infectious Diseases, Musashimurayama-shi, Tokyo 208-0011, the §§Department of Oral Histology, Nagasaki University Graduate School of Biomedical Sciences, 1-7-1 Sakamoto, Nagasaki 852-8588, Japan, and the ¶¶Otsuka Pharmaceutical Co., Ltd., Kagasuno 463-10 Kawauchi-cho, Tokushima 771-0192, Japan*

***Mycobacterium tuberculosis*** **infects not only host macrophages but also nonprofessional phagocytes, such as alveolar epithelial cells. Glycosaminoglycans (GAGs) are considered as the component of mycobacterial adherence to epithelial cells. Here we show that extracellularly occurring mycobacterial DNA-binding protein 1 (MDP1) promotes mycobacterial infection to A549 human lung epithelial cells through hyaluronic acid (HA). Both surface plasmon resonance analysis and enzyme-linked immunosorbent assay revealed that MDP1 bound to HA, heparin, and chondroitin sulfate. Utilizing synthetic peptides, we next defined heparin-binding site of 20 amino acids from 31 to 50 of MDP1, which is responsible for the specific DNA-binding site of MDP1. MDP1 bound to A549 cells, and exogenous DNA and HA interfered with the interaction. The binding was also abolished by treatment of A549 cells with hyaluronidase, suggesting that HA participates in the MDP1-A549 cell interaction. Adherence of bacillus Calmette-Guérin (BCG) and *M. tuberculosis* to A549 cells was inhibited by addition of HA, DNA, and anti-MDP1 antibody, showing that MDP1 participates in the interaction between mycobacteria-alveolar epithelial cells. Simultaneous treatment of intratracheal BCG-infected mice with HA reduced the growth of BCG *in vivo*. Taken together, theses results suggest that HA participates in *Mycobacterium*-lung epithelium interaction and has potential for therapeutic and prophylactic interventions in mycobacterial infection.**

Attachment of microbial pathogens to host cells is a critical event to develop mucosal infection (1). *Mycobacterium tuberculosis* persistently infects 32% of the world human population and is responsible for around 1.7 million deaths attributable to a single infectious pathogen each year (2). *M. tuberculosis* is transmitted by airborne particles and is deposited in a terminal alveolus, where the bacteria are phagocytosed by alveolar macrophages or invade into nonprofessional phagocytic cells such as epithelial pneumocytes (3, 4). Nonprofessional phagocytic cells are presumed to be hiding places of *M. tuberculosis* in persistent infection, because *M. tuberculosis* DNA can be frequently detected in type II alveolar epithelial cells and fibroblasts of the lung derived from tuberculin skin test-positive healthy individuals (5). However, the precise mechanism of the interaction between lung epithelial pneumocytes and mycobacteria remains unknown. Better understanding of the interaction is important for developing therapeutic/prophylactic strategies against tuberculosis.

Carbohydrates, such as glycosaminoglycans (GAGs),[1] are thought to be receptors in the process of mycobacterial infection to nonprofessional phagocytic cells (6). GAGs contain hyaluronic acid (HA), heparin, heparan sulfate, and chondroitin sulfates (7). Bacterial pathogens possess adhesion molecule, called adhesin to interact with host tissues. Heparin-binding hemagglutinin (HBHA) binds to GAGs and is identified as a mycobacterial adhesin in the mycobacterium-epithelial cell interaction (6). When bacillus Calmette-Guérin (BCG) or *M. tuberculosis* lacking HBHA was instilled into mice through the intranasal route, delay of extrapulmonary dissemination was observed (8). Thus interaction with epithelia is thought to be crucial for dissemination and to dominate the disease outcome. Besides HBHA, *M. tuberculosis* has another possible adhesin, designated mycobacterial cell entry protein 1 (Mcep1), of which DNA fragmentation confers on *Escherichia coli* an ability to invade into nonphagocytic HeLa cells (9), although its precise role as an adhesin remains unclear (10). It is likely that myco-

* This work was supported by grants from the Ministry of Health, Labour and Welfare (Research on Emerging and Re-emerging Infectious Diseases, Health Sciences Research Grants), The Japan Health Sciences Foundation, Ministry of Education Culture Sports Science and Technology, Inamori Foundation, Osaka City University (Urban Research Project), and The United States-Japan Cooperative Medical Science Program against Tuberculosis and Leprosy. The costs of publication of this article were defrayed in part by the payment of page charges. This article must therefore be hereby marked "*advertisement*" in accordance with 18 U.S.C. Section 1734 solely to indicate this fact.

§ To whom correspondence should be addressed. Tel.: 81-6-6645-3746; Fax: 81-6-6645-3747; E-mail: sohkichi@med.osaka-cu.ac.jp.

[1] The abbreviations used are: GAG, glycosaminoglycan; aa, amino acid; BCG, bacillus Calmette-Guérin; BSA, bovine serum albumin; fluos, 5(6)-carboxyfluorescein-*N*-hydroxysuccinimide ester; HA, hyaluronic acid; HBHA, heparin-binding hemagglutinin; GFP, green fluorescent protein; LBP, laminin-binding protein; MDP1, mycobacterial DNA-binding protein 1; P31–50, synthetic peptide corresponding to the amino acid sequence of MDP1 at the 31–50 position; RU, resonance units; SPR, surface plasmon resonance; CBB, Coomassie Brilliant Blue; CHO, Chinese hamster ovary cells; CFU, colony-forming units.

bacteria utilize multiple adhesins to promote attachment to nonprofessional phagocytes.

A number of nonspecific DNA-binding proteins are found in association with bacterial chromosomes and are called histone-like proteins. Mycobacterial DNA-binding protein 1 (MDP1) has a wide range of binding activities to genomic DNA through guanine and cytosine and is an abundant structural protein, which constitutes ~7% of cellular proteins in BCG and *M. tuberculosis* H37Rv (11). MDP1 possesses a DNA-binding site at the position of amino acids (aa) 31–50, the sequence of which does not exist in any other nucleic acid-binding protein (12). MDP1 has partial homology with HU, histone-like protein of *E. coli*, in the $NH_2$-terminal region and with eukaryotic histone H1 in the COOH-terminal region. These facts indicate that MDP1 is mycobacteria-specific histone-like protein (11). Importantly, MDP1 inhibits macromolecular biosyntheses of DNA, RNA, and protein *in vitro* and recombinant *E. coli* expressing MDP1 grows much slower when compared to the parental strain (13). The expression of MDP1 is up-regulated at the stationary or dormant phases of mycobacterial culture (11, 14). MDP1 and its homologues, which have been designated as histone-like protein (14) and laminin-binding protein (LBP) (15), are distributed in all mycobacterial species so far examined (12). These imply that MDP1 plays an important role in both slow growth and dormant/latent infection with mycobacteria.

Another interesting feature of this molecule is localization. MDP1 exits not only in the cytoplasmic space associated with the 50 S ribosomal subunit and presumably nucleoid but also on the bacterial surface (11, 15). Nuclear protein is localized in the cytoplasm, and its primitive roles are to compact the genome and control gene expression. However, some nuclear proteins are expressed on the cell surface and play alternative roles. For example, eukaryotic histone H1 on the cell membrane is identified as a receptor for thyroglobulin that is the precursor of thyroid hormones (16). High mobility group 1 protein is a eukaryotic nuclear protein associated with chromatin but also secreted in the extracellular milieu (17). Outside the cell, high mobility group 1 binds to the receptor for advanced glycation end products and then stimulates the cell damage signal. This signal eventually triggers inflammation for clearance of necrotic cells (18–20). *Mycobacterium leprae* produces LBP, which is a homologue of MDP1, although it lacks DNA-binding activity (15). Instead of DNA-binding activity, LBP interacts with laminin-2 and is considered to be involved in *M. leprae* invasion into Schwann cells of the peripheral nervous system (15).

The aim of this study was to clarify the role of surface-exposed MDP1 in the interaction between mycobacteria and lung epithelial cells, because DNA-binding proteins tend to bind GAGs that are thought to be receptors in the process of mycobacterial infection to nonprofessional phagocytes (6, 7). Our results demonstrate that extracellular MDP1 acts as an adhesin by binding to GAGs and mediates mycobacterial adherence to A549 human lung epithelial cells by interaction with hyaluronic acid (HA). Treatment of BCG-infected mice with HA resulted in the reduction of mycobacterial growth *in vivo*. Taken together, HA may play a key role in adherence of mycobacteria to lung epithelial cells.

## EXPERIMENTAL PROCEDURES

*Culture Medium and Reagents*—RPMI 1640 media, L-glutamine, and 0.05% trypsin EDTA solution, heparin from porcine intestinal mucosa, HA from human umbilical cord, and heparan sulfate from bovine kidney were purchased from Sigma. Chondroitin sulfate A and C were purchased from Calbiochem. Hyaluronidase from *Streptomyces hyaluronolytics*, heparinase 1 from *Flavobacterium heparinum*, and chondroitinase ABC from *Proteus vulgaris* were purchased from Sigma. Polyclonal anti-MDP1 sera were obtained from female rabbit (Japan SLC, Shizuoka, Japan) after multiple injections of MDP1 emulsified in incomplete Freund's adjuvant. Polyclonal anti-MDP1 antibodies were obtained by 30% ammonium sulfate precipitation of antisera. The salt was then removed by dialysis in PBS.

*Preparation of Subcellular Fractions of BCG*—To obtain subcellular fractions from BCG, all the following procedures were carried out at 4 °C. Ten grams of BCG was disrupted in cold PBS with a Bioruptor UCD-200T sonicator (Toso, Tokyo, Japan), and the suspension was centrifuged at 3,000 × *g* for 5 min to remove unbroken bacteria. The supernatant was centrifuged at 10,000 × *g* for 10 min. The pellet was rinsed with cold PBS and again centrifuged at 10,000 × *g* for 10 min. This cell wall-containing pellet was resuspended in 4 ml of cold PBS, and then Percoll (Amersham Biosciences) was added to be 60%. Next the mixture was centrifuged at 27,000 × *g* for 1 h to separate cell walls from unbroken cells. The cell wall band was collected and washed twice with PBS and was used as the cell wall fraction. A membrane-ribosome fraction was obtained by centrifugation of the supernatant of the cell wall-containing pellet at 105,000 × *g* for 2 h. The pellet and the supernatant were used as membrane-ribosome and cytoplasmic fractions, respectively. Culture supernatants of BCG were obtained filtration of culture media of BCG through the membrane filter (pore size of 0.22 μm) and concentrated by 80% of ammonium sulfate precipitation. The salt was then removed by dialysis in PBS. Twenty micrograms of each fraction was fractionated by SDS-PAGE, transferred to the polyvinylidene difluoride membrane, and reacted with polyclonal anti-MDP1 antisera.

*Immunogold Electron Microscopy*—BCG and *Mycobacterium smegmatis* were grown in Middlebrook 7H9-ADC media at 37 °C until $A_{1.5}$, and then the bacteria were collected by centrifugation. The bacterial pellet was fixed in 2.5% glutaraldehyde and 2% paraformaldehyde in phosphate buffer, pH 7.4, for 2 h at 4 °C and post-fixed in 1% osmium tetraoxide in the same buffer for 1 h at 4 °C. Specimens were dehydrated in graded ethanol and embedded in Epon-Araldite resin. The thin section was mounted on the nickel grids, treated in 3% $H_2O_2$ for 10 min, and washed in water. For blocking the nonspecific binding of antibody to the plastic, the section was preincubated with 3% BSA in PBS for 60 min at room temperature and washed by PBS, followed by incubation with rabbit anti-MDP1 antisera diluted in PBS containing 0.1% BSA and 0.05% Tween 20 (PBS-B-T, 1:800) for 2 h at room temperature. The section was then rinsed for 30 min and incubated with protein A conjugated with gold of 10 nm in diameter (EY Laboratories Inc., San Mateo, CA) diluted in PBS-B-T (1:100) for 1 h at room temperature. Finally, the section was rinsed with PBS and distilled water and then briefly stained with uranyl acetate and Reynolds' lead citrate. The section was analyzed using an H7100 electron microscope (Hitachi Co., Ltd., Tokyo, Japan) operated at 75 kV.

*Proteins Purification*—Native MDP1 and antigen 85B were purified from BCG strain Tokyo as described previously (11, 21). Recombinant MDP1 and HBHA were obtained as follows. Based on the nucleotide sequences of *mdp1* and *hbha*, the oligonucleotide primers, *i.e.* the forward (5′-CCCCATATGAACAAAGCAGAGCTCATTGAC-3′ and 5′-CATATGGCTGAAAACTCGAACAT-3′) and the reverse (5′-CCCAAGCTTTTTGCGACCCCGCCGAGCGG-3′ and 5′-AAGCTTCTGGGTGACCTTCTTG-3′) primers, were synthesized, respectively. The PCR was carried out by targeting 10 ng of chromosomal DNA derived from BCG in an automated thermal sequencer (Iwaki Glass Co., Tokyo, Japan). The samples were first denatured by heating at 94 °C for 5 min and then incubated for 30 cycles at 94 °C for 2 min, 56 °C for 80 s, and 72 °C for 5 min and then finally incubated for 5 min at 72 °C. The amplified DNA fragment, including *mdp1* and *hbha*, were digested by NdeI and HindIII, and inserted into the same sites of pET22b+ (Novagen, Darmstadt, Germany). These plasmids were designated pET22b-MDP1 and pET22b-HBHA, respectively. The DNA sequences of the cloned genes were confirmed by using an ABI 373 automatic DNA sequencer (Applied Biosystems, Foster, CA). The pET22b-MDP1 and pET22b-HBHA were introduced into *E. coli* BL21(DE3)pLys (Invitrogen), and these recombinant bacteria were harbored in LB media containing 50 μg/ml carbenicillin and 34 μg/ml chloramphenicol at 22 °C. When an optical density at 600 nm of the culture reached 0.3–0.6, isopropyl-1-thio-β-D-galactopyranoside was added to a final concentration of 0.1 mM, and then the mixture was incubated for additional 7 h. The cells were sonicated as described above, and the supernatant was collected after centrifuging 8,000 × *g* for 30 min. After removing the clamp from the supernatant by filtration through a 0.22-μm membrane filter, it was applied to a 1-ml Hi-Trap chelating column previously charged with 100 mM $NiSO_4$ and equilibrated with 20 mM sodium phosphate, pH 7.4, 10 mM imidazole, and 0.5 M NaCl. After unbound proteins were washed

out, the protein was eluted with the same buffer containing 300 mM imidazole. The fractions containing MDP1 were collected and dialyzed against PBS. The purity of proteins was confirmed by SDS-PAGE analysis and stained with Coomassie Brilliant Blue R-250 (CBB) as a single band.

*Heparin-Sepharose Chromatography*—An MDP1-rich, acid-soluble protein fraction was obtained from BCG as described before (11). 200 μg of acid-soluble protein was fractionated by heparin-Sepharose chromatography (Amersham Biosciences), of which bed volume was 1 ml, at room temperature with a linear gradient of NaCl in PBS. Gradients were made in a gradient apparatus filled with 10 ml each of 0.15 and 2 M NaCl solution. A flow rate of 1 ml/min was maintained, and 1 ml of each fraction was collected. The fraction was analyzed by SDS-PAGE. The protein bands were stained with CBB.

*Surface Plasmon Resonance Measurements*—The interaction between MDP1 and GAGs was monitored by measuring SPR using a BIAcore 2000 biosensor (BIAcore AB, Uppsala, Sweden). All binding reactions were performed at 25 °C in 10 mM HEPES buffer, pH 7.4, including 150 mM NaCl, 3 mM EDTA, and 0.005% surfactant P20. Proteins and peptide were immobilized to the dextran matrix on the CM5 sensor chip (BIAcore) using an amine coupling kit according to the manufacturer's instructions (BIAcore). Association and dissociation rate constants were calculated by nonlinear fitting of the primary sensorgram data using BIAevaluation software version 3.0.

*Determination of the Heparin-binding site by ELISA*—20-mer of synthetic sequential peptides corresponding to the amino acid sequence of MDP1 (12) were immobilized on the 96-well ELISA plate (Sumitomo, Osaka, Japan) at a concentration of 10 μg/ml in carbonate buffer, pH 9.6, at 4 °C overnight. After blocking the wells by 5% BSA in PBS, biotinylated heparin (Sigma) was added at 1 μg/ml in PBS containing 0.05% Tween 20 (PBS-T) to each well and incubated for 1 h at 37 °C. After washing unbound heparin, horseradish peroxidase-conjugated streptavidin was added and the mixture was incubated for 1 h at 37 °C. After washing free streptavidin, binding was detected by color development with *o*-phenylendiamine dihydrochloride (Wako, Tokyo, Japan), and ELISA units (optical density) were measured at 492 nm.

Inhibition of interaction between MDP1 and heparin by the synthetic peptide was examined by the following procedure. MDP1 was immobilized on the 96-well ELISA plate at a concentration of 4 μg/ml in carbonate buffer, pH 9.6, at 4 °C overnight. Biotinylated heparin and peptide were premixed in PBS-T for 10 min at 37 °C and added into each MDP1-immobilized well. After 30-min incubation at 37 °C, unbound heparin was washed out and the level of binding was determined by horseradish peroxidase conjugated with streptavidin as described above.

*Detection of MDP1 Binding to GAGs by ELISA and Inhibition Assay by Exogenous DNA*—Genomic DNA of BCG and HA were immobilized on the 96-well ELISA plate at 10 μg/ml and heparin and chondroitin sulfate C were done at 100 μg/ml overnight incubation at 37 °C. MDP1 at 1 μg/ml in PBS-T was added into wells and incubated for 1 h at 37 °C. Wells were washed, and then anti-MDP1 antisera diluted by PBS-T to 1 to 1000 were added. After 1-h incubation at 37 °C, wells were washed and peroxidase-conjugated anti-rabbit antibody was added. After washing the wells, MDP1 binding was detected by color development with *o*-phenylendiamine dihydrochloride as described above.

*Protein Labeling*—MDP1 was labeled with 5(6)-carboxyfluorescein-*N*-hydroxysuccinimide ester (fluos, Roche Diagnositics GmbH, Mannheim, Germany). One milligram of MDP1 was mixed with 0.237 mg of fluos in 1 ml of PBS for 2 h at room temperature. The molar ratio of fluos to MDP1 is 10 to 1. Then, nonreacted fluos was separated by gel filtration on the Sephadex G-25 column (Amersham Biosciences). Similarly, bovine serum albumin (BSA, Sigma) and HBHA were labeled with fluos (molar ratio, 10 to 1). Concentrations of labeled proteins were determined by Bradford's method (22) using BSA as a standard.

*Protein Binding Assay to A549 Type II Human Lung Epithelial Cells*—A549 cells were suspended at $2 \times 10^5$ cells/ml in RPMI 1640 medium containing 10% fetal bovine serum (Sigma), 25 mM HEPES, 2 mM L-glutamine, $5.5 \times 10^{-5}$ M 2-mercaptoethanol (complete culture medium), and 1 ml of cell suspensions was dispensed into individual wells of a 24-well plate (BD Biosciences). Plates were incubated at 37 °C in a humidified atmosphere at 5% $CO_2$ for 24 h. The nonadherent cells were poured off, and the residual nonadherent cells were removed by washing with serum-free RPMI 1640 medium twice and refilled with 200 μl of complete culture medium. fluos-labeled MDP1, BSA, or HBHA was added to a final concentration of 0.5 μM, and the mixture was incubated for 0–5 h. In experiments of enzymatic treatment, epithelial cells were treated with heparinase 1, hyaluronidase, or chondroitinase ABC (Sigma) before incubation with proteins. One unit of each enzyme was added into each well and incubated for 2 h in PBS at 37 °C under 5% $CO_2$. Then enzymes were removed by washing with PBS twice and incubated with fluos-labeled proteins. After the incubation, wells were washed three times with RPMI 1640 medium at 37 °C to remove nonadherent proteins. Then cells were detached by using cell scrapers and collected in a tube and centrifuged at 300 × *g* for 5 min. After removing supernatant, cells were fixed by adding 1 ml of 1% paraformaldehyde-PBS. Fixed cells were analyzed by flow cytometry using Cellquest™ software (BD Biosciences).

*Construction of Mycobacteria Expressing Green Fluorescent Protein*—A BamHI-EcoRI 0.7-kbp fragment from the vector pEGFP (BD Biosciences) containing the gene encoding GFP was introduced into the *E. coli*-mycobacteria shuttle vector pMV261 (23) to generate the plasmid pMV261GFP. This plasmid was introduced into BCG by electroporation, and kanamycin-resistant BCG colonies were selected after 3 weeks of culture on Middlebrook 7H11 agar containing oleic acid, dextrose, albumin, and catalase enrichment (Difco, 7H11-OADC agar) in the presence of 20 μg/ml kanamycin. The expression of GFP was confirmed by confocal laser microscopy LSM510 (Carl Zeiss, Tokyo, Japan) according to the manufacturer's instructions.

*Experimental Infection in Vitro*—Mycobacterial suspension was prepared by the conventional method (24) after harvesting bacteria in 7H9 media (Difco) supplemented with 10% albumin, dextrose, and catalase enrichment (Difco) and 0.05% Tween 80 at 37 °C until 0.6 of optical density at 650 nm. Bacterial suspensions were added to A549 epithelial cells at multiplicities of infection ranging from 1 to 10 bacteria/epithelial cell. After either 6- or 24-h incubation, unbound bacteria were washed with RPMI 1640 medium three times, and adherent epithelial cells were collected by scraping with rubber policeman. Serial 10-fold dilutions of the cell suspension were cultivated on 7H11-OADC agar. Colonies were counted after 3 weeks incubation at 37 °C. Cells infected with BCG expressing GFP were assessed by flow cytometry (FACScan, BD Biosciences) as described in the fluos-labeled protein binding assay.

*Experimental Infection in Vivo*—Female C57BL/6 mice, 7 weeks of age (Japan Clea, Suita, Osaka, Japan), were challenged intratracheally with $1 \times 10^6$ CFUs of BCG in the presence or absence of 50 μg of HA. At 2 weeks of infection, lungs of mice were removed aseptically and homogenized individually with a set of motor and pestle. The homogenate was plated on 7H11-OADC agars after 10-fold serial dilution. Mycobacterial colonies were counted 3 weeks after the culture.

*Statistical Analyses*—Data were analyzed by Power Macintosh G4 using StatView 5.0 (SAS Institute Inc., Cary, NC) and expressed as the mean ± S.D. Data that appeared statistically significant were compared by an analysis of variance for comparing the means of multiple groups and considered significant if $p$ values were less than 0.05.

## RESULTS

*Cellular Localization of MDP1*—We examined cellular localization of MDP1 by both biochemical and ultrastructural analyses. Subcellular fractions obtained from BCG were examined by Western blot analysis by anti-MDP1 antisera (Fig. 1*A*). The result showed anti-MDP1 antibody reacted with the bands in the cell wall and the membrane-ribosome fractions. In contrast, antibody failed to react with cytoplasmic fraction and culture filtrates. Next immunogold electron microscopic examination was carried out. Protein A-coupled with gold particles did not react with the section (Fig. 1*B*). In contrast, anti-MDP1 antibody reacted with both inside and outside mycobacteria (Fig. 1*C*). These results indicate that MDP1 localizes on/in the cell wall as well as intracellular ribosome and membrane fractions. This agrees with previous findings (11, 15).

*Amino Acids Sequence Homology between MDP1 and HBHA*—Sequence alignments among BCG-MDP1, *M. tuberculosis*-MDP1, and *M. tuberculosis*-HBHA were carried out by a malign program through the DNA data base of Japan (Fig. 2). BCG-MDP1 revealed a lack of nine amino acids from *M. tuberculosis*-MDP1, and the identity of amino acid sequences was 95%. The total sequence homology between MDP1 and HBHA was low (BCG-MDP1 and HBHA, 35%; *M. tuberculosis*-MDP1 and HBHA, 34%), although both proteins possessed the conserved region in the C-terminal (Fig. 2). HBHA possessed a heparin-binding site in the C-terminal region, and four PAKK repetitive sequences are key residues for binding to GAGs (25,

26). Six PAKK repetitive sequences were seen in the C-terminal region of MDP1 (Fig. 2).

*MDP1 Binds to Heparin*—To explore the role of extracellularly occurring MDP1, we examined the binding capacity of MDP1 to heparin. Acid-soluble proteins enriched MDP1 derived from BCG (11) were applied on heparin-Sepharose chromatography, and heparin-binding proteins were fractionated by chromatography with a linear gradient from 0.15 to 2 M NaCl (Fig. 3*A*). Major 28-kDa protein on SDS-PAGE analysis was eluted by the fraction peak at 11 that was equivalent to 1 M NaCl. This protein was confirmed as MDP1 by Western blotting analysis utilizing monoclonal antibody (data not shown) and by determining the N-terminal amino acid sequences. It was reported that HABA was eluted at around 0.3 M NaCl by heparin-Sepharose column chromatography (26). Thus MDP1 is likely to bind to heparin with stronger affinity comparing to HBHA.

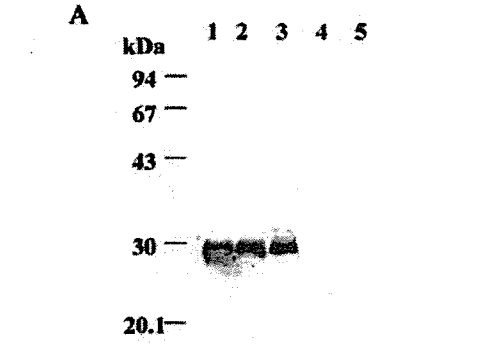


FIG. 1. **Cellular localization of MDP1 in mycobacteria.** *A*, subcellular localization of MDP1 analyzed by the Western blot. Subcellular fractions were reacted with anti-MDP1 antisera on the transferred membrane after fractionated by SDS-PAGE. *Lanes*: *1*, cell lysate of BCG; *2*, cell wall fraction; *3*, membrane-ribosome fraction; *4*, cytoplasmic fraction; *5*, culture filtrate. *B* and *C*, immunogold electron microscopic examination. *B*, control, pre-immune rabbit sera reaction. *C*, anti-MDP1 antisera reaction. Magnification factor is ×20,000. *Bar*, 1 μm.

*SPR Analysis of the Interaction between MDP1 and GAGs*—To clarify the molecular interaction between MDP1 and GAGs, SPR analysis was performed. In the preliminary experiment, we found that MDP1 bound to both basic sensor chip C1 and dextran-coated sensor chip CM5. Based on this result, we subjected MDP1 as an immobilized ligand in the subsequent experiments.

Native MDP1 and antigen 85B, a 28-kDa fibronectin-binding protein (27, 28), were immobilized on the CM5 sensor chip until gaining 3332 and 3312 resonance units (RUs), respectively. Heparin (10 μg/ml), as an analyte, was injected into the control sensor cell and immobilized cells with either MDP1 or antigen 85B for 20 s. As expected from the result of heparin-Sepharose column chromatography analysis, the interaction between MDP1 and heparin was observed until gaining 300 RU. Heparin did not interact with antigen 85B and empty sensor.

To know whether MDP1 binds to possible receptors for mycobacteria in adherence to epithelial cells, we extended the study to other GAGs. It was previously reported that, in addition to heparin, adherence to Chinese hamster ovary (CHO) cells was inhibited by chondroitin sulfate, but not dextran, mannose, and galactose (6). Accordingly we examined these carbohydrates by SPR analysis. The results showed that chondroitin sulfate A, and chondroitin sulfate C bound to MDP1. The gaining maximum RUs were 63 and 55, respectively. In contrast, other carbohydrates such as dextrose, mannose, galactose, arabinose, and trehalose did not bind to MDP1 (data not shown). These data show that MDP1 binds to certain GAGs that are possible receptors for adherence to CHO cells (6). Also, MDP1 bound to HA and heparan sulfate with 90 and 89 RU, respectively (data not shown). All carbohydrates tested failed to bind to empty sensor or antigen 85B immobilized sensor cells.

Next we attempted to determine the affinity between MDP1 and GAGs. Because of the limitation of employing GAGs of certain molecular size, affinities were determined for heparin ($M_r$ 5,000, Fig. 3*B*) and heparan sulfate ($M_r$ 10,000, Fig. 3*C*) (Table I). Because true binding affinity cannot be determined for the ligand with multivalent, pseudo apparent rate constants ($k_a$ and $k_d$) were calculated by the basic model. The affinity ($K_D$) of heparin and heparan sulfate was $3.53 \times 10^{-10}$ and $1.54 \times 10^{-8}$, respectively.

Previously, real-time association between HBHA and heparin was studied by SPR analysis (26). In comparison to that, MDP1 associates with heparin more quickly and dissociates more slowly (HBHA to heparin, $k_a$: $5.62 \times 10^5$ $M^{-1}$ $s^{-1}$, $k_d$:

```
BCG-MDP1  MNK----------AELIDVLTQKLGSDRRQATAAVENVVDTIVRA  35
Mtb-MDP1  MNK----------AELIDVLTQKLGSDRRQATAAVENVVDTIVRA  35
Mtb-HBHA  MAENSNIDDIKAPLLAALGAADLALATVNELITNLRERAEETRTDTRSRVEESRARLTKL  60
          *                    ***  *     *     **

BCG-MDP1  VHKGDSVTITGFGVFEQRRRAARVARNPRTGETVKVKPTSVPAFRPGAQFKAVVSGAQRL  95
Mtb-MDP1  VHKGDSVTITGFGVFEQRRRAARVARNPRTGETVKVKPTSVPAFRPGAQFKAVVSGAQRL  95
Mtb-HBHA  QEDLPEQLTELREKFTAEELRKAAEGYLEAATSRYNELVERGEAALERLRSQQSFEEVSA  120
                  *

BCG-MDP1  PAEGPAVKRGVGASAAKKVAKKAPAKKATKAAK---------KAATKAPAKKAATKAPAK  146
Mtb-MDP1  PAEGPAVKRGVGASAAKKVAKKAPAKKATKAAKKAATKAPARKAATKAPAKKAATKAPAK  155
Mtb-HBHA  RAEGYVDQAVELTQEALGTVASQTRAVGERAAK---------LVGIELPKKAAPAKKAA-  170
           ***       *          ***                 * * *  *  *

BCG-MDP1  KAVKATKSPAKKVTKAVKKTAVKASVRKAATKAPAKKAAAKRPATKAPAKKATARRGRK  205
Mtb-MDP1  KAVKATKSPAKKVTKAVKKTAVKASVRKAATKAPAKKAAAKRPATKAPAKKATARRGRK  214
Mtb-HBHA  --------PAKKAA----------PAKKAAAKKAPAKKAAAKKVTQ--------K  199
                  ****              * ** **** **  * *           *
```

FIG. 2. **MDP1 and HBHA possess PAKK repetitive sequences in the C-terminal regions.** The alignment of amino acid sequences allowing gaps (−) between MDP1 (BCG-MDP and *M. tuberculosis*-MDP1) and HBHA. The alignment was performed by malign program through DDBJ DNA data base. *Asterisks* indicate conserved aa among three proteins. *Blue* and *underlined* sequences represent the MDP1-specific DNA binding region previously determined (8). Repetitive aa sequences, PAKK, are highlighted by *red*. *Mtb*, *M. tuberculosis*.

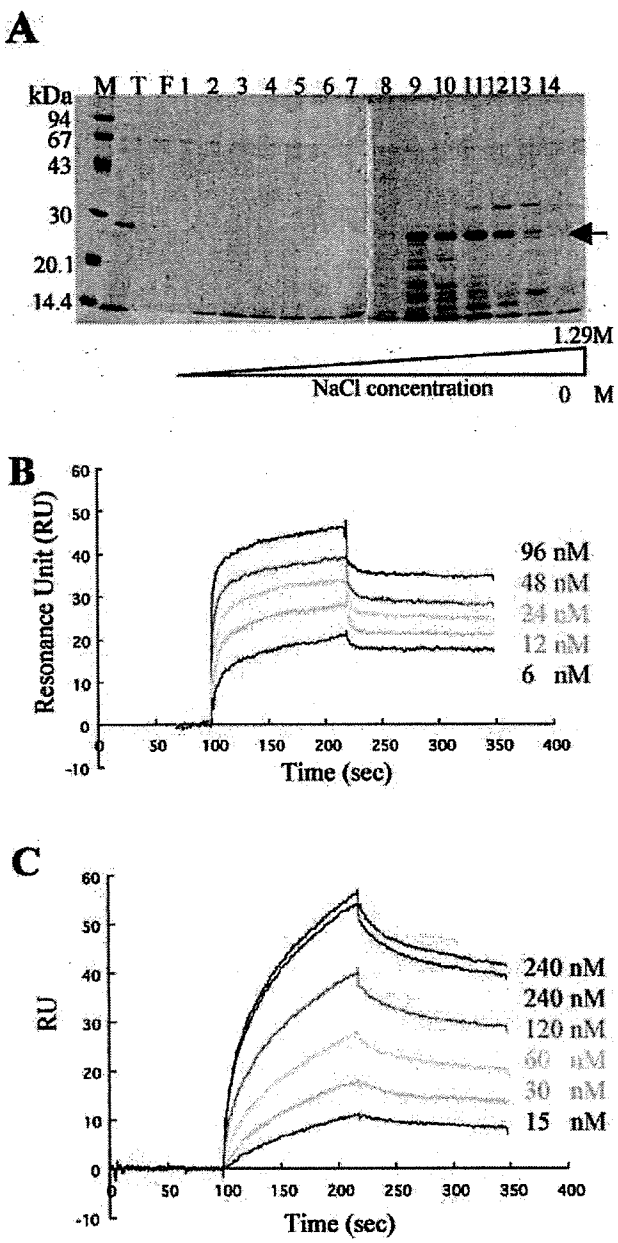


FIG. 3. **MDP1 binds to GAGs.** *A*, size fractionation of elutriates from heparin-Sepharose chromatography by SDS-PAGE. The gel was stained with CBB. *M*, molecular weight markers. *T*, total acid-soluble proteins applied to chromatography. *F*, unbound flow-through fraction. The *arrow* indicates MDP1. *B* and *C*, surface plasmon resonance analysis of the interaction between MDP1 and GAGs. Results for heparin (*B*) and heparan sulfate (*C*) are shown. Each GAG was injected at different concentrations as indicated in the figures and flowed over a surface chip at flow rate of 10 μl/min. RU values are the subtracted values of empty sensor cells from MDP1 immobilized sensor cells.

$1.5 \times 10^{-2}$, $K_D$: $2.6 \times 10^{8}$). The results of the heparin column study (Fig. 3*A*) and SPR analysis (Fig. 3*B*) indicate that MDP1 possesses much higher affinity to heparin than HBHA.

*Determination of the Heparin-binding Site of MDP1*—The difference of affinity between MDP1 and HBHA may be explained by binding sites other than PAKK repetitive regions in MDP1. To determine the binding site, we examined the heparin-binding activity of 20-mer of synthetic peptides covering the entire sequence of MDP1 (12). Wells of microtiter plates were coated with synthetic peptides and reacted with biotin-labeled

TABLE I
*Kinetics parameters for MDP1-GAG interaction from SPR analysis*

| Immobilized ligand | Analytes | Association rate, $k_a$ | Dissociation rate, $k_d$ | Affinity, $K_D$ |
|---|---|---|---|---|
| | | *1/ms* | *1/s* | *M* |
| MDP1 | Heparin | $1.08 \times 10^{6}$ | $3.83 \times 10^{-4}$ | $3.53 \times 10^{-10}$ |
| | Heparan sulfate | $9.81 \times 10^{4}$ | $1.51 \times 10^{-3}$ | $1.54 \times 10^{-8}$ |

heparin. Heparin bound to the peptide corresponding to an amino acid sequence of MDP1 at the 31–50 position (P31–50) (Fig. 4).

To exclude errors due to variation of the level of immobilization among peptides, inhibition assay was carried out. Only P31–50 inhibited the binding of heparin to MDP1 (molar ratio, heparin/peptide = 1/100, data not shown). On the contrary, the peptides containing PAKK did not interfere with the interaction between MDP1 and heparin. But this is not controversial, because longer amino acid sequences involving more than three PAKK sequences is required for binding of HBHA to heparin (26). Next we tried to determine the affinity between P31–50 and heparin by SPR analysis. P31–50 bound to both CM5 and C1 sensor chips as MDP1 did. Therefore, P31–50 was subjected to the ligand and immobilized on the CM5 sensor chip until gaining 3015 RU. Injection of heparin (30 s, 10 μg/ml) into P31–50-immobilized cells gained 91 RU, confirming binding activity of P31–50 to heparin, although we could not determine the $K_D$ value by using the BIAevaluation software. For this reason, a large part of the binding site of synthetic peptide may be inactivated and/or masked during immobilization procedure.

*Exogenous DNA Inhibits MDP1-GAG Interaction*—To provide direct evidence that MDP1 shares DNA- and GAG-binding sites, an inhibition assay was carried out by ELISA. As expected from SPR analysis, binding of MDP1 to GAG was detected as shown in Fig. 5. Binding of MDP1 to GAGs was inhibited by exogenous DNA, similar to the inhibition of MDP1-DNA interaction by DNA (Fig. 5). These results have confirmed the binding activity of MDP1 to GAGs and also showed that MDP1 interacts with GAGs by its DNA-binding site.

*MDP1 Binds to A549 Human Lung Epithelial Cells*—To know whether MDP1 binds to epithelial cells, A549 cells were incubated with fluos-labeled MDP1, fluos alone, and fluos-labeled BSA served as controls. Confocal laser microscopic analysis showed MDP1 (Fig. 6*A*), but not fluos alone and BSA (data not shown), attached to cells. The kinetics and magnitude of the binding were monitored after adding a final concentration of 0.5 μM MDP1 or HBHA by using flow cytometry (Fig. 6*B*). Binding of MDP1 to A549 cells were seen immediately after the addition of MDP1, conspicuous by 10 min, and reached a plateau by 60 min after the addition. More than 95% of A549 cells were MDP1-positive 60 min after. By contrast, binding of HBHA was delayed and more than 10% of cells were HBHA-negative even at the plateau.

To know whether MDP1 binding to A549 cell is dependent on GAGs, the following experiments were performed. First we examined the inhibitory effects of exogenously added GAGs. Addition of either heparin or HA resulted in a dose-dependent and remarkable inhibition of binding, whereas mannose did not (Fig. 6*C*). In contrast, heparin and HA partially inhibited interaction between HBHA and A549 cell, and thus the level of interference was much less comparing to MDP1 (Fig. 6*D*). Next, we determined which GAG actually participates in MDP1 binding to A549 cells utilizing enzymes degrading GAGs. Heparinase 1 degrades heparin, heparin sulfate, and HA (29), and chondroitinase ABC degrades chondroitin sulfate and HA (30). Hyaluronidase derived from *Streptomyces* is specific for HA unlike other hyaluronidases (31). Treatment of

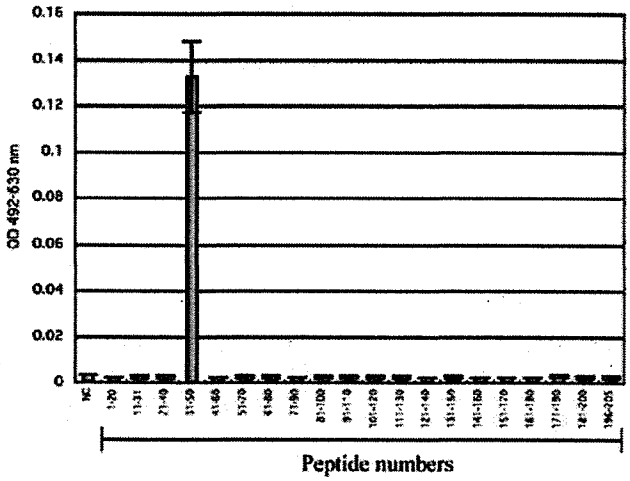


FIG. 4. **The MDP1-specific DNA binding region is the heparin-binding site.** Each peptide corresponding to the amino acid sequence of MDP1 was immobilized, and then biotinylated heparin was reacted. *OD*, optical density; *NC*, negative control without peptide.

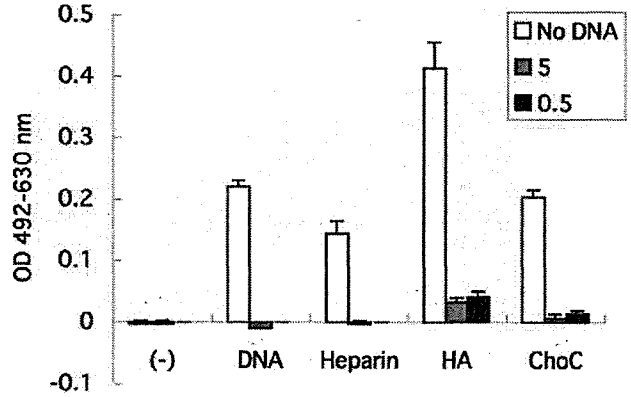


FIG. 5. **DNA interferes with MDP1-GAG interaction.** The wells of ELISA plates were coated with DNA and GAGs, and then MDP1 was added in the presence or absence of exogenous DNA. The level of MDP1 binding was determined by ELISA utilizing anti-MDP1 antisera. *ChoC*, chondroitin sulfate C. *No DNA*, without exogenous DNA. 5 or 0.5 $\mu$g of DNA was added to the wells as inhibitors.

A549 cells with these enzymes resulted in a reduction of the binding (untreated, 93.0%; treated with heparinase 1, 38.5%; chondroitinase ABC, 26.8%; hyaluronidase, 5.8%; and the combination of enzymes, 3.7%) (Fig. 7.) These results indicate that MDP1 binds to HA on A549 cells.

*Inhibition of MDP1-A549 Cell Interaction by Exogenous DNA*—We have already demonstrated that the DNA-binding region of MDP1 interacts with heparin (Figs. 4 and 5). The result prompted us to examine the possibility that the region may participate in the binding to A549 epithelial cells. The addition of exogenous DNA inhibited the binding of MDP1 (Fig. 8), but not HBHA (data not shown), to A549 cells. Based on the fact that MDP1 and its fragment, P31–50, bound to DNA via guanine and cytosine (11), we examined the effect of oligonucleotide DNA with 20-mer of dideoxyguanine (poly(dG)) on the interaction between MDP1 and A549 cells. The binding was inhibited by the addition of oligonucleotide DNA, although the intensity was less than plasmid DNA (Fig. 8). Taken together, these results suggest that MDP1 can bind A549 epithelial cells with its DNA-binding site.

*Involvement of MDP1 and GAG Interaction in the Attachment/Invasion of Mycobacteria to A549 Cells*—To elucidate the role of MDP1 in the attachment/invasion of mycobacteria, A549 epithelial cells were infected with BCG expressing GFP *in vitro*. CFUs determination showed around 7% of inoculated bacteria bound to cells after 6-h incubation. The interaction was then visualized by confocal laser microscopy. The result showed around 60% of bacteria bound to cells and 40% was invaded. Thus BCG not only bound to but also invaded into cells. This was consistent with previous reports (4, 32). In this condition, exogenous HA, heparin, DNA, and anti-MDP1 antibodies inhibited the interaction between GFP-expressing BCG and A549 cell (Fig. 9*A*). P31–50 suppressed BCG-A549 cell interaction as well (data not shown). Among these, the most potent inhibitor of the interaction was HA. Similar results were obtained from the experiment involving *M. tuberculosis* (Fig. 9*B*).

*Inhibition of BCG Growth in Vivo by Treatment of Mice with HA*—We have extended *in vitro* studies to *in vivo* animal experiments regarding the inhibitory role of GAGs in the interaction. Mice were injected intratracheally with either $1 \times 10^6$ CFU of BCG alone or BCG plus 50 $\mu$g of HA. Two weeks after the challenge, 40,875 ± 16,585 CFU was recovered from the lung of BCG-infected mice (Fig. 10). Treatment of such mice with HA resulted in a marked reduction of BCG growth (5,960 ± 4,530 CFU). This result was consistent with that of *in vitro* study, probably due to the prevention of mycobacterial attachment/invasion by exogenous HA.

## DISCUSSION

The bacterial chromosomes are associated with abundant histone-like proteins that compactly hold the genome (33–35). It is generally accepted that such histone-like proteins participate functionally in the regulation of gene expression by altering three-dimensional genome structure (33–35). MDP1 is a presumed mycobacteria-specific histone-like protein, although it localizes on the cell wall, besides inside the cell (11, 15). In the present study we have focused on the physiological role of extracellularly occurring MDP1. We postulated that surface-exposed MDP1 acts as an adhesin in *Mycobacterium*-epithelial cell interaction based on the following facts. First, GAG is estimated as an infectious site of mycobacteria to epithelial cells (6). Second, DNA-binding protein tends to bind GAGs, as for example the heparin-Sepharose column is conventionally used to purify nuclear proteins. Third, MDP1 possesses six PAKK sequences that represent the heparin-binding site of HBHA (Fig. 2).

In the present study we explored interaction between MDP1 and GAGs and found that MDP1 directly bound to GAG at the DNA-binding site (Figs. 3–5). Affinity was determined by SPR analysis. Apparent rate constants were calculated by the basic model, because heparin and heparan sulfate are multivalent. There is a discrepancy at least in part by difference between the fitted model and real interaction mechanism and requires further investigation to obtain the actual kinetic constants for the interaction. MDP1 bound to A549 lung epithelial cells mainly through cell surface HA (Fig. 7). Anti-MDP1 antibody treatment inhibited the binding of mycobacteria, including BCG and *M. tuberculosis*, to A549 cells (Fig. 9). These findings indicate that MDP1 acts as an adhesin in the interaction with lung epithelial cells of the host. To our knowledge, this study demonstrates for the first time that bacterial pathogen utilizes extracellular DNA-binding proteins to attach host cells.

It has also been known that HBHA binds to GAGs and is identified as a mycobacterial adhesin (6). MDP1 and HBHA are structurally distinct proteins, although both proteins possess the conserved repetitive PAKK sequences in the C terminus (Fig. 2). Functionally, MDP1 binding to A549 cells was seen immediately after its addition, and >95% of A549 cells were MDP1-positive 60 min thereafter. In contrast, binding of HBHA was delayed, and >10% of cells were HBHA-negative

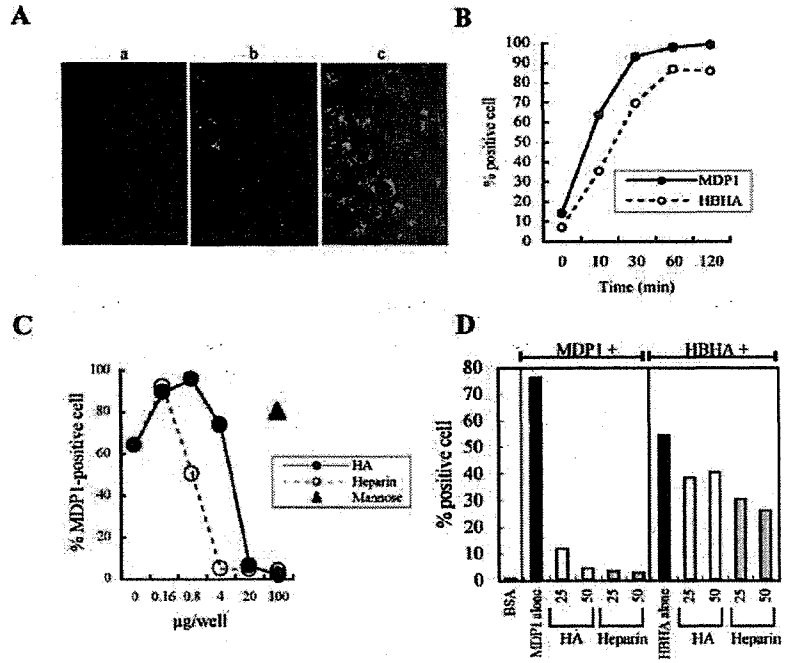


FIG. 6. **MDP1 binds to A549 human lung epithelial cells.** *A*, phase contrast microscopic image (*a*) and corresponding fluorescent microscopic image (*b*). *c*, merge of *a* and *b*. *B*, binding kinetics of MDP1 and HBHA to A549 cells. fluos-labeled MDP1 (0.5 μM) was incubated with A549 cells for 1 h. MDP1- and HBHA-bound cells were determined by FACScan at each time point after the addition of proteins (*horizontal axis*). *C*, heparin and HA, but not mannose, inhibited the binding of MDP1 to A549 cells. MDP1 was pre-incubated with HA, heparin, and mannose and was then added into the culture of A549 cells. After 2-h incubation, the % of MDP1-bound cells was determined by FACScan. *D*, inhibition by HA and heparin of the binding of MDP1 (*left panel*) and HBHA (*right panel*) to A549 cells.

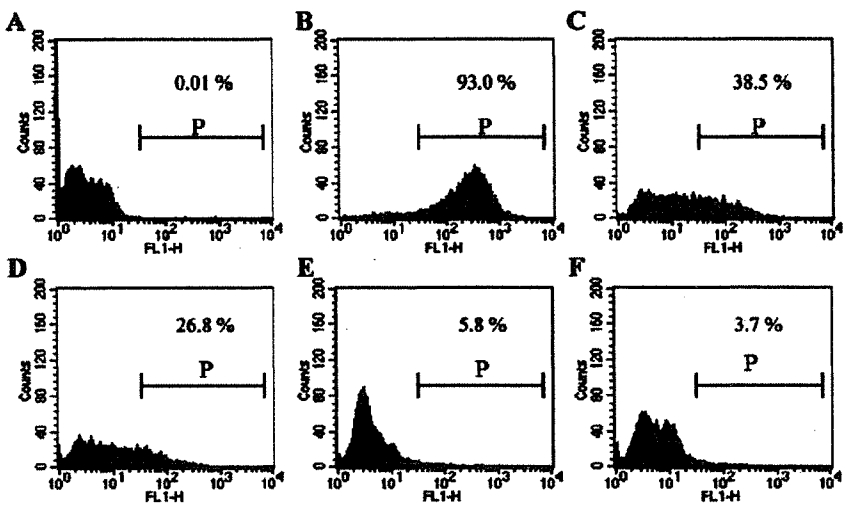


FIG. 7. **MDP1 binds to A549 cells through HA.** Untreated A549 cells bound to fluos-BSA served as negative controls (*A*) and to fluos-MDP1 as positive controls (*B*). MDP1 was added to the culture of cells pretreated with heparinase 1 (*C*), chondroitinase ABC (*D*), hyaluronidase (*E*), and combination of these three enzymes (*F*). Intensity of fluorescence was determined by FACScan 4–5 h after the culture.

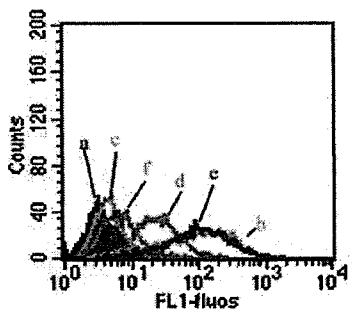


FIG. 8. **DNA interferes in MDP1-A549 cell interaction.** A549 cells were incubated with fluos-BSA (*a*, *purple*), fluos-MDP1 alone (*b*, *green*), fluos-MDP1 plus plasmid DNA (pBSKS+) (*c*, *light blue*), synthetic poly(dG) (*d*, *pink*), rabbit control immunoglobulins (*e*, *dark blue*) (Sigma), rabbit anti-MDP1 polyclonal antibodies (*f*, *orange*) for 2 h. The binding was monitored by FACScan.

even at the plateau phase (Fig. 6*B*). The possible mechanism of the functional difference can be explained by the affinity experiment, which showed that MDP1 possessed stronger binding activity to GAGs than HBHA, as assessed by heparin Sepharose column chromatography and BIAcore biosensor analysis (Fig. 3) (26). Another possible mechanism is the distinct binding site of MDP1 and HBHA to GAGs. The binding site of MDP1 comprises aa 31–50, which is the DNA binding region, but not the region of six repetitive sequences of PAKK in its C terminus (Fig. 4), whereas that of HBHA comprises four repetitive sequences of PAKK (20, 21). As expected, exogenous DNA inhibited the binding of MDP1, but not HBHA, to A549 cells (Fig. 8 and data not shown). The interaction between MDP1 and A549 cells was through cell surface HA (Fig. 7), whereas heparan sulfate is presumed to be the site for HBHA (26).

Another major difference between MDP1 and HBHA is their localization. MDP1 retained mycobacterial cell walls, although HBHA is released to the extracellular milieu. The nature of MDP1 having strong affinity to both cell walls and GAG may be more favorable than HBHA to attach to host tissues. Recently Coutte *et al.* (36) found that the release of adhesin to the extracellular milieu is necessary for efficient colonization of *Bordetella pertussis*, which colonizes to the human respiratory

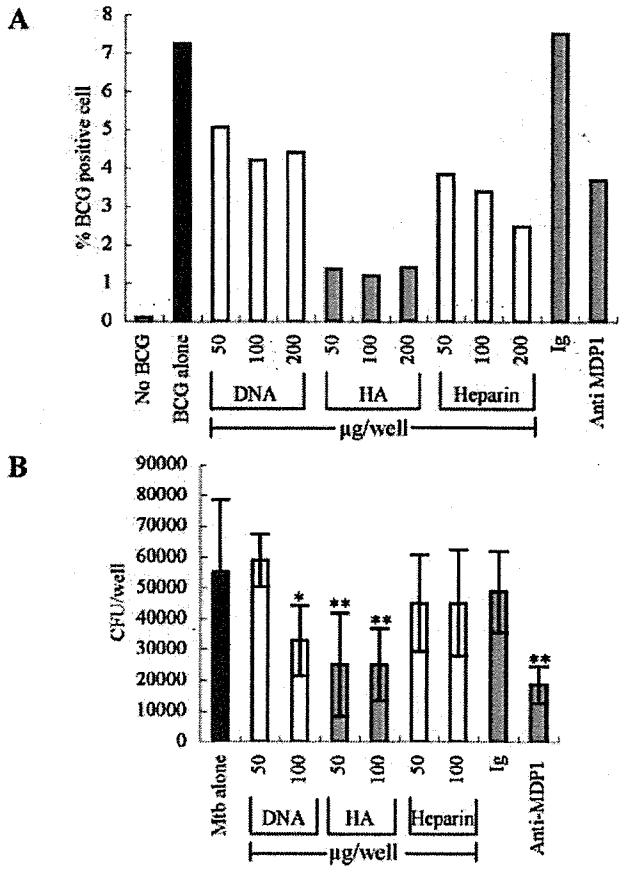


FIG. 9. **MDP1 is involved in the attachment/binding of mycobacteria to A549 cells.** *A*, the attachment/binding of BCG expressing GFP to A549 cells. BCG were pretreated with DNA, anti-MDP1 antibodies, HA, and heparin, and were then added into the culture of A549 cells. As controls for antibody experiments, rabbit control Ig (Sigma) was added. The binding was assessed by FACScan. The average of duplicated samples was presented. *B*, CFU of *M. tuberculosis* pretreated with GAGs and anti-MDP1 antibodies recovered from the coculture with A549 cells. Bacterial numbers were counted 3 weeks after the culture on the Middlebrook 7H11 agars. *Mtb*, *M. tuberculosis*. *, $p < 0.05$ and **, $p < 0.01$ as compared with Mtb alone by analysis of variance.

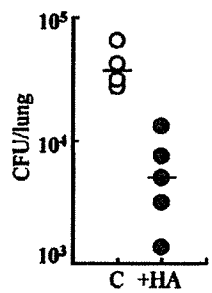


FIG. 10. **Inhibition of infection of BCG *in vivo* by treatment of mice with HA.** C57BL/6 mice were challenged intratracheally with either $1 \times 10^6$ CFU BCG alone (*C*) or BCG plus 50 μg of HA (+*HA*). All results are expressed as individual mouse data. *Bars* indicate averages. $p = 0.0143$ as compared between two groups by Mann-Whitney *U* test.

tract. HBHA induces bacterial aggregation, thereby mediating bacteria-bacteria interaction (6). These reports suggest that exported HBHA participates in the dispersal of bacteria from microcolonies for the spread of infection. This hypothesis explains the important finding by Pethe *et al.* (8): delay of dissemination of HBHA-lacking BCG and *M. tuberculosis* from the lung to spleen. Taking these considerations together, mycobacteria possess at least structurally and functionally two distinct adhesion proteins, such as extracellular MDP1 and HBHA.

It remains uncertain how MDP1 is expressed on cell walls of mycobacteria. An MDP1 gene does not encode signal sequence of secretion, and it does not contain the transmembrane domain of integration into the cell membrane. However, the large amounts of MDP1 that were localized on/in mycobacterial cell walls (Fig. 1) imply that some machinery is present that transports MDP1 outside the cell membrane rather than retention on the cell surface due to cell lysis of bacteria. Certain proteins that lack signal sequence and a transmembrane domain, such as ESAT-6 (37), CFP-10 (38), HSP65 and superoxide dismutase (SOD) (39, 40), and glutamine synthetase (39), are actively exported from mycobacteria and play significant roles in the pathogenesis. Further study is needed to clarify the issue of transportation of MDP1.

Hyaluronidase treatment of A549 cells abolished MDP1-A549 cell interaction (Fig. 7), and exogenous addition of HA reduced the binding of BCG and *M. tuberculosis* to A549 cells (Fig. 9), suggesting that cell surface HA is the key GAG for adherence of mycobacteria to lung epithelial cells. Mycobacterial adhesins other than MDP1 are likely to participate in binding to HA, because anti-MDP1 antibodies and DNA, inhibited the interaction between mycobacteria and A549 cells less than HA (Fig. 9*A*).

Based on the results of *in vitro* experiments, we have attempted the therapeutic intervention by HA using experimental infection with BCG in mice. Treatment of such mice with HA resulted in a marked reduction of BCG growth in the lung (Fig. 10). The results support the *in vitro* study that HA plays an important role in the interaction between mycobacteria and lung epithelial cells. This suggests that HA has potential for prophylactic interventions in mycobacterial infection.

HA has so far received little attention in the research of host-*Mycobacterium* interaction. HA is a polymer comprising repeating disaccharide units of (β1→4)D-glucuronate-(β1→3)*N*-acetyl-D-glucosamine (7). HA is the major component of the extracellular matrix and acts as a signaling molecule for cells depending on their size (41, 42). Professional phagocytes, such as macrophages, and professional antigen presenting cells, such as dendritic cells, play important roles in defense against mycobacterial infection in the lung (43). HA modulates the functions of dendritic cells and macrophages (42). Fragmented HA, which accumulates during inflammation, stimulates nitric oxide production (44), which is the major bactericidal effector against *M. tuberculosis* (43, 45). Furthermore, CD44, a major receptor of HA (46, 47), is recently identified as the site of mycobacterial entry to macrophages (48). We focused mainly on mycobacteria-epithelial cell interaction in this study, and our findings imply that HA plays an important role in interactions between mycobacteria and macrophages/dendritic cells. The precise mechanism of the interaction remains to be elucidated, and such study is currently underway in our laboratory.

*Acknowledgments*—We gratefully acknowledge Drs. Yukiko Nishiuchi, Shinji Maeda, and Clifton E. Barry III for helpful suggestions. We also acknowledge Mika Egami, Yasuyoshi Nishio, and Yukimi Kira in the technical assistances of fluorescein microscopy, flow cytometry, and BIAcore sensor analysis. In addition, we thank Megumi Matsumoto, Sara Matsumoto, and Takeshi Yamada for their heartfelt encouragement.

REFERENCES

1. Kagnoff, M. F., and Eckmann, L. (1997) *J. Clin. Invest.* **100**, 6–10
2. Bloom, B. R. (2002) *N. Engl. J. Med.* **346**, 1434–1435
3. Small, P. M., and Fujiwara, P. I. (2001) *N. Engl. J. Med.* **345**, 189–200
4. Bermudez, L. E., and Goodman, J. (1996) *Infect. Immun.* **64**, 1400–1406
5. Hernandez-Pando, R., Jeyanathan, M., Mengistu, G., Aguilar, D., Orozco, H., Harboe, M., Rook, G. A., and Bjune, G. (2000) *Lancet* **356**, 2133–2138

6. Menozzi, F. D., Rouse, J. H., Alavi, M., Laude-Sharp, M., Muller, J., Bischoff, R., Brennan, M. J., and Locht, C. (1996) *J. Exp. Med.* **184,** 993–1001
7. Hardingham, T. E., and Fosang, A. J. (1992) *FASEB J.* **6,** 861–870
8. Pethe, K., Alonso, S., Biet, F., Delogu, G., Brennan, M. J., Locht, C., and Menozzi, F. D. (2001) *Nature* **412,** 190–194
9. Arruda, S., Bomfim, G., Knights, R., Huima-Byron, T., and Riley, L. W. (1993) *Science* **261,** 1454–1457
10. Shimono, N., Morici, L., Casali, N., Cantrell, S., Sidders, B., Ehrt, S., and Riley, L. W. (2003) *Proc. Natl. Acad. Sci. U. S. A.* **100,** 15918–15923
11. Matsumoto, S., Yukitake, H., Furugen, M., Matsuo, T., Mineta, T., and Yamada, T. (1999) *Microbiol. Immunol.* **43,** 1027–1036
12. Furugen, M., Matsumoto, S., Matsuo, T., Matsumoto, M., and Yamada, T. (2001) *Microb. Pathog.* **30,** 129–138
13. Matsumoto, S., Furugen, M., Yukitake, H., and Yamada, T. (2000) *FEMS Microbiol. Lett.* **182,** 297–301
14. Lee, B. H., Murugasu-Oei, B., and Dick, T. (1998) *Mol. Gen. Genet.* **260,** 475–479
15. Shimoji, Y., Ng, V., Matsumura, K., Fischetti, V. A., and Rambukkana, A. (1999) *Proc. Natl. Acad. Sci. U. S. A.* **96,** 9857–9862
16. Brix, K., Summa, W., Lottspeich, F., and Herzog, V. (1998) *J. Clin. Invest.* **102,** 283–293
17. Muller, S., Scaffidi, P., Degryse, B., Bonaldi, T., Ronfani, L., Agresti, A., Beltrame, M., and Bianchi, M. E. (2001) *EMBO J.* **20,** 4337–4340
18. Yang, T., Witham, T. F., Villa, L., Erff, M., Attanucci, J., Watkins, S., Kondziolka, D., Okada, H., Pollack, I. F., and Chambers, W. H. (2002) *Cancer Res.* **62,** 2583–2591
19. Andersson, U., Wang, H., Palmblad, K., Aveberger, A. C., Bloom, O., Erlandsson-Harris, H., Janson, A., Kokkola, R., Zhang, M., Yang, H., and Tracey, K. J. (2000) *J. Exp. Med.* **192,** 565–570
20. Scaffidi, P., Misteli, T., and Bianchi, M. E. (2002) *Nature* **418,** 191–195
21. Naito, M., Ohara, N., Matsumoto, S., and Yamada, T. (1998) *Scand. J. Immunol.* **48,** 73–78
22. Bradford, M. M. (1976) *Anal. Biochem.* **72,** 248–254
23. Stover, C. K., de la Cruz, V. F., Fuerst, T. R., Burlein, J. E., Benson, L. A., Bennett, L. T., Bansal, G. P., Young, J. F., Lee, M. H., and Hatfull, G. F., Snapper, S. B., Barletta, R. G., Jacobs, W. R., and Bloom, B. R. (1991) *Nature* **351,** 456–460
24. Molloy, A., Laochumroonvorapong, P., and Kaplan, G. (1994) *J. Exp. Med.* **180,** 1499–1509
25. Delogu, G., and Brennan, M. J. (1999) *J. Bacteriol.* **181,** 7464–7649
26. Pethe, K., Aumercier, M., Fort, E., Gatot, C., Locht, C., and Menozzi, F. D. (2000) *J. Biol. Chem.* **275,** 14273–14280
27. Naito, M., Ohara, N., Matsumoto, S., and Yamada, T. (1998) *J. Biol. Chem.* **273,** 2905–2909
28. Janicki, B. W., Chaparas, S. D., Daniel, T. M., Kubica, G. P., Wright, G. L., and Yee, G. S. (1971) *Am. Rev. Respir. Dis.* **104,** 602–604
29. Yang, V. C., Bernstein, H., Cooney, C. L., and Langer, R. (1987) *Appl. Biochem. Biotechnol.* **16,** 35–50
30. Yamagata, T., Saito, H., Habuchi, O., and Suzuki, S. (1968) *J. Biol. Chem.* **243,** 1523–1535
31. Ohya, T., and Kaneko, Y. (1970) *Biochim. Biophys. Acta* **198,** 607–609
32. McDonough, K. A., and Kress, Y. (1995) *Infect. Immun.* **63,** 4802–4811
33. Drlica, K., and Rouviere-Yaniv, J. (1987) *Microbiol. Rev.* **51,** 301–319
34. Pettijohn, D. E. (1988) *J. Biol. Chem.* **263,** 12793–12796
35. Schmid, M. B. (1988) *Trends Biochem. Sci.* **13,** 131–135
36. Coutte, L., Alonso, S., Reveneau, N., Willery, E., Quatannens, B., Locht, C., and Jacob-Dubuisson, F. (2003) *J. Exp. Med.* **197,** 735–742
37. Sorensen, A. L., Nagai, S., Houen, G., Andersen, P., and Andersen, A. B. (1995) *Infect. Immun.* **63,** 1710–1717
38. Berthet, F. X., Rasmussen, P. B., Rosenkranda, I., Andersen, P., and Gicquel, B. (1998) *Microbiology* **144,** 3195–3203
39. Harth, G., and Horwitz, M. A. (1999) *J. Biol. Chem.* **274,** 4281–4292
40. Braunstein, M., Espinosa, B. J., Chan, J., Belisle, J. T., and Jacobs, W. R., Jr. (2003) *Mol. Microbiol.* **48,** 453–464
41. Camenisch, T. D., Spicer, A. P., Brehm-Gibson, T., Biesterfeldt, J., Augustine, M. L., Calabro, A., Jr., Kubalak, S., Klewer, S. E., and McDonald, J. A. (2000) *J. Clin. Invest.* **106,** 349–360
42. Termeer, C., Sleeman, J. P., and Simon, J. C. (2003) *Trends Immunol.* **24,** 112–114
43. Flynn, J. L., and Chan, J. (2001) *Annu. Rev. Immunol.* **19,** 93–129
44. McKee, C. M., Lowenstein, C. J., Horton, M. R., Wu, J., Bao, C., Chin, B. Y., Choi, A. M., and Noble, P. W. (1997) *J. Biol. Chem.* **272,** 8013–8018
45. Chan, J., Xing, Y., Magliozzo, R. S., and Bloom, B. R. (1992) *J. Exp. Med.* **175,** 1111–1122
46. Turley, E. A., Noble, P. W., and Bourguignon, L. Y. (2002) *J. Biol. Chem.* **277,** 4589–4592
47. Cichy, J., Pure, E., Turley, E. A., Noble, P. W., and Bourguignon, L. Y. (2003) *J. Cell Biol.* **161,** 839–843
48. Leemans, J. C., Florquin, S., Heikens, M., Pals, S. T., van der Neut, R., and Van Der Poll, T. (2003) *J. Clin. Invest.* **111,** 681–689

Jpn.J.Leprosy 73, 263-270(2004)

# 抗酸菌病原因子と宿主応答の分子機序

小林　和夫*
大阪市立大学大学院医学研究科感染防御学

〔受付：2004年7月6日〕

キーワード：血清診断、抗酸菌DNA結合蛋白質、宿主防御、細胞壁表層糖脂質、病変形成

抗酸菌感染症には結核、非結核性抗酸菌感染症やハンセン病などがあり、現在でも、多くの抗酸菌感染症患者が存在し、人類に甚大な健康被害を提供している。全世界では約20億人（全人口の1/3）が結核菌に既感染、毎年800万人が結核を発病、200万人が死亡している。今後10年間、少なくとも、8,000万人が発病、2,000万人が死亡することが推定されている。結核菌の病原性として、1）宿主防御機構からの逸脱や2）遅延型過敏反応（細胞性免疫応答の負の側面）の誘導があり、その結果、結核菌感染から発病に至る長期の潜伏期間、組織破壊を伴う肉芽腫炎症が特徴的である。結核菌病原因子として、細胞壁表層構成成分が関与していると考えられている。病原因子として、1）細胞壁表層糖脂質、2）lipoarabinomannan、3）補体活性化因子、4）熱ショック蛋白質や5）抗酸菌DNA結合蛋白質などがあり、これらの因子は抗酸菌や宿主に対する多機能分子である。抗酸菌感染症の制圧には抗酸菌病原因子や宿主応答の分子機序の解明、さらに、この機序の解明は新規治療戦略やワクチン開発に寄与するであろう。

## はじめに

世界の年間総死亡は約5,400万人、その内訳として、循環器疾患（虚血性心疾患や脳血管障害など）：1,670万人、感染症：1,350万人、悪性新生物：700万人であり、感染症は現在でも全世界の総死亡の約1/4を占め、人類に大きな健康被害を招来している。感染症による死亡（1,350万人／年）の主要な原因として、急性呼吸器感染症（肺炎など）：396万人、後天性免疫不全症候群（AIDS、結核の合併を含む）：267万人、下痢性疾患：220万人、結核：200万人、マラリア：109万人や麻疹：89万人などがある（表1）。

抗酸菌感染症には結核、非結核性抗酸菌（nontuberculous mycobacteria：NTM）感染症やハンセン病などがあり、現在でも、多くの抗酸菌感染症患者が存在し、人類に甚大な健康被害を提供している。全世界では約20億人（全人口の1/3）が結核菌（*Mycobacterium tuberculosis*）に既感染、毎年800万人が結核を発病、200万人が死亡し、有病者は2,200万人である。今後10年間、少なくとも、8,000万人が発病、2,000万人が死亡することが推定されている。日本（2002年）では年間3.3万人（罹患率人口10万対：25.8）が結核を発病し、2.3千人（死亡率：1.8）が死亡し、有病者は3.2万人（有病率：25.4）、結核は単一病原体による感染症として、世界最大である。結核対策の課題として、1）急速な人口の高齢化に伴う高齢者結核の増加（70歳以上の占める割合：約40%）、

*Corresponding author：
〒545-8585　大阪府大阪市阿倍野区旭町1-4-3
TEL：06-6645-3745　FAX：06-6646-3662
E-mail：kobayak@med.osaka-cu.ac.jp
Web site：http://www.med.osaka-cu.ac.jp/hostdefense